DEVELOPMENT OF A STERILIZABLE RUGGEDIZED VIDICON FOR LUNAR AND PLANETARY PHOTOGRAPHY

Interim Technical Report

Period Covered

21 May 1965 through 21 August 1966

Contract No. 950985

Prepared for

California Institute of Technology
JET PROPULSION LABORATORIES
4800 Oak Grove Drive
Pasadena, California

Prepared by

S A Ochs

S. A. Ochs
Project Engineer

Approved by

F D Marschka

F. D. Marschka
Project Supervisor

Approved by

R W Engstrom

R. W. Engstrom
Manager, Advanced Development

Prepared by

Electronic Components and Devices
RADIO CORPORATION OF AMERICA
Industrial Tube and Semiconductor Division
Lancaster, Pennsylvania

September 1966

Foreword

This report was prepared by Radio Corporation of America, Electronic Components and Devices, Industrial Tube and Semiconductor Division, Lancaster, Pennsylvania, under JPL Contract No. 950985. The JPL Project Engineers were L. Ralph Baker and Henry Canvel.

This Interim Report covers the period from May 21, 1965 to August 21, 1966. The work was performed in Conversion Tube Operations, D. W. Epstein, Manager; Advanced Development Section, R. W. Engstrom, Manager. F. D. Marschka was the Project Supervisor and S. A. Ochs the Project Engineer. The following engineers also contributed to the work described in this report: J. L. Rhoads, J. G. Ziedonis, W. M. Kramer, R. L. Blazek and J. A. Zollman. The fabrication and testing of components and tubes was done with the assistance of D. D. Neuer.

TABLE OF CONTENTS

		Page
	Task I	
I.	PHOTOCONDUCTOR DEVELOPMENT	1
II.	STERILIZATION AND DECONTAMINATION	2
III.	TESTING	3
	A. Dark Current Vs. Target Voltage	3
	B. Signal Current Vs. Target Voltage	3
	C. Light Transfer Characteristic	4
	D. Spectral Characteristics	4
	E. Resolution	4
	F. Grey-Scale Rendition	4
	G. Erasure	4
IV.	EXPERIMENTAL RESULTS	5
	A. Dark Current	5
	B. Sensitivity	15
	C. Light Transfer Characteristics	15
	D. Spectral Response	19
	E. Resolution	19
	F. Gray-scale	23
	G. Erasure	23
V.	DISCUSSION	23

TABLE OF CONTENTS

		Page
	Task II	
I.	DESIGN	28
II.	MANUFACTURE OF TUBES	33
III.	ENVIRONMENTAL TESTING AND FAILURE ANALYSIS	38
IV.	PERFORMANCE	50
V.	SUMMARY AND CONCLUSIONS	53

LIST OF FIGURES

Figure		Page
1	Distribution of Tubes in Terms of Dark Current After Sterilization to Initial Dark Current	10
2	Distribution of Tubes in Terms of Dark Current After Sterilization to Initial Dark Current	11
3	Semilog Plot of Dark Current (of Five Tubes) Vs. Temperature	13
4	Semilog Plot of Dark Current (of Three Tubes) Vs. Target Voltage, Before and After Dry-Heat Sterilization	14
5	Distribution of Tubes in Terms of Sensitivity (Signal Current at 1.0 ft-cd Target Illumination) After Sterilization to Initial Sensitivity	16
6	Semilog Plot (for Two Tubes) of Signal Current at 1.0 ft-cd Target Illumination Vs. Target Voltage	17
7	Distribution of Tubes, Before and After Sterilization, in Terms of Gamma	18
8	Light Transfer Curve of Tube No. 22 at Slow-Scan Rate	20
9	Average Spectral Response (of 11 Tubes) Before and After Sterilization	21
10	Distribution of Tubes, Before and After Sterilization, in Terms of Resolution	22
11	Distribution of Tubes, Before and After Sterilization, in Terms of Gray-Scale Rendition	24

LIST OF FIGURES
(CONT'D.)

Figure		Page
12	Distribution of Tubes, Before and After Sterilization, in Terms of Residual Signal at Third Scan After Removal of Light	25
13	Semilog Plot of Average Dark Current and Average Signal Current at 1.0 ft-cd Faceplate Illumination Vs. Target Voltage, Before and After Sterilization	27
14	External and Cross Sectional View of Complete (Unpotted) Ceramic Vidicon	29
15	Ceramic Vidicon	30
16	Cross Sectional View of Gun Section of Ceramic Vidicon	32
17	Ceramic Cathode Structure	34
18	External View of Ceramic Vidicon as Potted in Magnetic Shield	35
19	Centrifuge for Constant Acceleration Test	39
20	Vibration Test Unit	40
21	High Acceleration Shock Machine and Detail of Drop Table (with holding fixture)	42
22	Oscilloscope Trace of Typical Shock Pulse	43
23	Heater Test Assembly	47
24	Dark Current Vs. Target Voltage for Ceramic Vidicon	51
25	Signal Current Vs. Target Voltage for Ceramic Vidicon	52
26	Signal Current Vs. Faceplate Illumination for Ceramic Vidicon	54
27	Spectral Response of Ceramic Vidicon	55
28	Amplitude Response of Ceramic Vidicon	56

ABSTRACT

A one inch vidicon was developed which can withstand ethylene-oxide and dry-heat sterilization as well as exposure to severe shock and vibration. The tube has a ceramic-metal modular construction and is potted in a magnetic shield. Electrostatic focusing and deflection are employed. Tubes successfully passed through the sterilization treatment and environmental testing. Electrical performance is encouraging with resolution of over 500 TV lines having been observed.

Objective

The first phase of Contract No. 950985 covered a 15-month research and development project for a sterilizable, ruggedized vidicon. Task I of this contract comprised a 10-month program for developing a photoconductor suitable for use in this camera tube. More specifically, the objective of Task I was to develop and demonstrate a photoconductor capable of giving satisfactory performance after having undergone the required dry-heat sterilization and gas decontamination compatibility tests.

The objective of Task II is to build a tube which incorporates the photoconductor developed in Task I and which is ruggedized to withstand the vibration and shock environment of a missile launch and the impact shock of a landing spacecraft.

I. PHOTOCONDUCTOR DEVELOPMENT

The development of a sterilizable slow-scan photoconductor followed the general outline presented in proposal DP 5132 as amended.

The substrate used consisted of vitreous quartz of extremely high quality as far as surface defects were concerned. The faceplates were selected according to their freedom from visible imperfections when viewed by microscope of 30X magnification under light of grazing incidence. Although the inspection criterion was a complete absence of visible imperfections, few substrates in actual fact met this specification.

The initial tubes made on this project were already very promising as far as general performance and resistance to dry-heat sterilization were concerned. However, they showed up a serious problem of spottiness. White, grey and black spots were visible in the television picture and appeared to be caused by imperfections in the photoconductor layer. Attempts at removing this problem included: (1) improvement of the vacuum conditions during the photoconductor evaporation, (2) improved filtering of the inert gas which is admitted to the system upon completion of the evaporation, (3) shortening the time during which the photolayer is exposed to air before exhaust of the tube on which it is mounted, and (4) improved faceplate preparation. Although all of these measures may have contributed to the reduction of spurious signals, it became increasingly clear during the course of the project that the chief source of spottiness lay in the faceplate cleaning procedures.

Repeated re-evaluation and improvements of the faceplate washing and drying procedures resulted in a very substantial reduction of spottiness. Although this problem cannot be considered as having been completely solved, spurious signals were reduced to the point where they are only of secondary importance.

No evidence was observed of any increase in spottiness due to the sterilization procedures.

The final faceplate cleaning procedure decided upon consisted of the following steps: (1) Wash substrates in a water solution of Alconox detergent by swabbing with cotton balls, (2) Rinse substrates in hot deionized water and, then, in cold deionized water, (3) Follow with a closely controlled rinsing and drying procedure in a vapor dryer charged with isopropyl alcohol.

The degree of cleanliness of the substrates at this stage was preserved as closely as possible until the faceplate was loaded in the evaporator. It is not likely that any appreciable contamination could occur during this interval since the cleaning facilities and the evaporator are both located in the same clean room.

The evaporations were performed in a dry pumping system evacuated by sorption and ion pumps without the use of organic vapors. The jigging was designed such that the signal electrode and the photoconductive layer could be deposited without breaking vacuum. Because of the above, the substrate was not exposed to air from the time it was loaded into the evaporator to completion of the photosurface. Therefore, the possibility of contamination occurring between the signal plate and the photoconductor was minimized.

The application of glow-discharge cleaning was evaluated. It appeared that this process was not needed for producing the desired photoconductor characteristics or for good layer adherence to the substrate. Since glow-discharge cleaning was considered as the possible cause of some gross spots found in early tubes, it was decided not to continue to use this cleaning method any further.

The signal electrode (back plate) used in all tubes consisted of rhodium which was evaporated from a rhodium-plated tungsten-wire heater. The resistance of the signal electrodes, as monitored on test slides, varied between 90K and 900K ohms per square. Tube performance appeared to be independent of variations in signal-electrode resistance so long as the resistance was below one megohm per square. The optical transmisssion of a rhodium coating as used in this work is approximately 65 to 70% relative to air.

The photolayer used was of the RCA developed ASOS type. Since electrical performance changed so little with the sterilization bakes, an elaborate program of photoconductor development was not necessary. Only a minor modification in the evaporation schedule was made (at tube No. 11) in order to effect a slight decrease in dark current, although it does not appear that an appreciable change was caused. Except for this small adjustment, all evaporations were made using essentially the same evaporation profile.

The finished faceplates were removed from the evaporator, inspected optically and then mounted in RCA 7735A vidicons. These commercial tubes are 1" vidicons with magnetic focus and deflection. Their heater operates at 6.3 volts and 0.6 amperes.

II. STERILIZATION AND DECONTAMINATION

Dry-heat sterilization of the experimental tubes was performed in accordance with JPL Spec. XSO-30275-TST-A, "Environmental Test Specification Compatibility Test for Planetary Dry-Heat Sterilization Requirements."

The vidicons were baked in an electrically-heated air-tight chamber provided with a dry nitrogen atmosphere. Up to 8 tubes were treated simultaneously. The tubes rested on Teflon supports inside a stainless steel box which was placed in the heating chamber. The temperature was monitored by two or

three chromel-alumel thermocouples, which were usually placed in contact with the faceplate rings of different tubes. A separate thermocouple placed in contact with the stainless steel box was connected to a Brown Electronik recording controller which regulates the electric power for heating the chamber.

During a typical heating cycle, the temperature of the experimental tubes was raised to 145°C plus or minus 2°C and maintained there for 36 hours. At the end of the cycle the tubes were allowed to stabilize at room temperature. In all cases, several hours or days elapsed between heating cycles.

For the ethylene-oxide decontamination, tubes were placed in the air-tight chamber and exposed to an atmosphere containing twelve percent ethylene-oxide and 88 percent Freon 12, by weight. The relative humidity was controlled as per paragraphs 3.5 and 3.6.1 of JPL Specification GMO50198-ETS. The temperature was kept at 40°C and monitored as described above. The required amount of water was metered with a pipette and injected into the chamber through a stopcock. The vidicons exposed to this test were treated for 24 hours.

III. TESTING

The vidicons were tested at standard television rate, 60 fields per second interlaced, with 525 lines per frame. A raster of 0.48" width and 0.36" height was scanned. The following measurements were made:

A. Dark Current Vs. Target Voltage

Readings were taken at successively higher values of target voltage (usually to 60V). For each reading, the electron beam was increased until it was just able to discharge the target surface. The current was measured with a Keithley 414 micro-microammeter. Due to the slow response of the meter, it took considerable time for equilibrium to be established at any given target voltage. In order to obtain meaningful results within a practical time, all dark current readings were taken one minute after the target was first discharged at the particular target voltage in question.

The temperature of the faceplate was found to be an important parameter influencing dark current. Therefore, in many tests, the faceplate temperature was monitored with a thermocouple and attempts were made to keep the faceplate at a constant temperature by means of a flow of cooled air.

B. Signal Current Vs. Target Voltage

The sensitivity of the photoconductor was measured in terms of the signal current due to a faceplate illumination of one footcandle. Readings were taken at different target voltages increasing in steps of 10V, as long as sufficient electron beam was available.

C. Light Transfer Characteristic

Signal current was measured as a function of faceplate illumination (at intensities of 0.01, 0.10 and 1.0 footcandle) with the faceplate at 20V. The gamma of the photoconductor, i.e. the slope of the characteristic when plotted on log-log coordinates, was then measured.

D. Spectral Characteristics

The tube was operated at a target voltage of 20V and the uniform target illumination adjusted to the value yielding a signal current of 0.200 uA. Narrow band optical filters were then interposed between the light source and the target, and the corresponding signal current was measured for each wavelength. A correction factor was then applied to each measurement to make allowance for the brightness of the tungsten light source at the wavelength in question and for the transmission of the particular filter used.

E. Resolution

A EIA resolution pattern was projected onto the faceplate. With the target at 20V, the light intensity was varied until a signal current of 0.200 uA was produced. The beam was decreased in magnitude until it was just able to discharge the highlight portions on the target.

The ultimate resolution was measured in the central region of the target and at the corners. In some cases, the beam focus was readjusted between these two readings so as to give optimum resolution. This procedure was adopted since the resolution capability of the photoconductor, rather than that of the beam, was desired.

F. Grey-Scale Rendition

The dynamic range of the tubes was measured in terms of the number of grey-scale steps which could be recognized on the EIA resolution pattern. The same operating parameters were used as for the measurement of resolution.

G. Erasure

The erase characteristics of the tubes were measured in terms of the signal remaining at the third scan after the removal of uniform illumination. The tube was operated at a pre-determined target voltage, usually 20V, and the light intensity adjusted such that the signal current was 0.200 uA. The lower half of the faceplate was then masked so that a reference black level signal was produced.

A chopper, located between the light source and the tube, interrupted the light for one-third of a second every second. The signal output was displayed on an oscilloscope and the lag measured in terms of the signal produced at the third scan after the light had been interrupted.

IV. EXPERIMENTAL RESULTS

A total of fifty-one vidicons were made. Six of these did not receive the three sterilization cycles and final test: One (#11) had too many spots to be useful; three (#15, 22, 23) were overheated during the sterilization procedure so that the indium faceplate seal melted and vacuum was lost; the glass bulbs of two tubes (#27, 47) cracked during the second bake cycle.

Table I shows some of the data obtained from these fifty-one tubes. It can be seen that the changes in the various characteristics caused by the dry-heat sterilization procedure are far from consistent and are relatively small compared to the variations from tube to tube. However, certain significant features emerge quite clearly and provide a basis for predicting the effect of the sterilization process on any given tube.

A. Dark Current

Dark current, at a fixed target voltage, was considered the tube characteristic which would be most susceptible to change under the sterilization procedure. Table II shows the distribution of 45 vidicons as to change in dark current at two target voltages. At each value of the ratio

$$\frac{\text{Dark Current after Sterilization}}{\text{Initial Dark Current}}$$

the number of tubes is given for which this ratio was obtained. The same data are displayed graphically in Figs. 1 and 2, for target voltages of 20V and 30V, respectively.* Here the abscissas represent the dark current ratio, divided into segments of width 0.3. For instance, the segment marked 1.7 includes the values of the dark current ratio in the range from 1.55 to 1.85. The ordinates indicate the number of tubes belonging to each segment. Smooth curves were drawn which approximate this distribution of the experimental tubes.

*The dark currents of tubes No. 25 and 26 at E_t = 20V were so small that the measurements were very inaccurate. The entries for these two tubes in Fig. 1, therefore, were based on the dark currents measured at E_t = 30V.

Table I

Selected Data from Experimental Vidicons
Before and After Three Sterilization Bakes

NG	Dark Current (E_t = 20V) Initial	Dark Current (E_t = 20V) Final	Signal Current (E_t = 20V, Ill. = 1 fc) Initial	Signal Current (E_t = 20V, Ill. = 1 fc) Final	Resolution (E_t = 20V, IS = 200 uA) Initial	Resolution (E_t = 20V, IS = 200 uA) Final	Residual Signal (at third scan, E_t = 20V) Initial	Residual Signal (at third scan, E_t = 20V) Final	Grey-Scale Initial	Grey-Scale Final	Gamma Initial	Gamma Final
1	4.2 nA	3.7 nA	259 nA	315 nA	600 lines	600 lines	80%	80%	8 steps	8 steps	0.55	0.63
2	5.0	7.0	265	350	500	600	80	81	8	8	.60	.64
3	6.7	10.0	514	480	600	500	80 (E_t=30V)	77	8	10	.70	.75
4	3.0	14.3	418	555	600	550	82(E_t=15V)	83	-	10	.70	.67
5	8.0	11.5	392	454	500	425	74(E_t=30V)		10	10	.72	.70
6	11.0	15.0	489	440	500	425	79		10	10	.65	.67
7	4.5	4.0	400	400	650	550	76		10	10	.73	.75
8	2.0	4.6	340	390	650	525	72		10	10	.71	.80
9	2.9	4.5	350	360	550	350	80		10	10	.65	.62
10	4.3	5.5	420	400	550	350	81		10	10	.66	.65
11									not tested, very bad spots			
12	5.6	29.0	375	500		350	76			7	.69	.71
13	7.5	10.0	423	540	650	600	82		10	10	.70	.72
14	3.4	8.5	447	512	550	375	82		10	8	.70	.66
15	6.5		500		500		80		10		.70	
16	2.0	1.9	303	428	400	400	80	75	10	7	.70	.68
17	0.7	2.5	285	422	450	375	82	79	10	7	.66	.70
18	3.9	6.0	366	460	500	600	78	78	8	10	.74	.77
19	2.7	3.0	367	440	550	600	80	76	8	10	.77	.72
20	7.2	9.0	433	611	500	425	80	78	8	10	.74	.69
21	6.5	10.0	474	630	200	400	81	80	8	10	.73	.68
22	<.01		450		550		86		7		.68	

Table I (Cont'd.)

NG	Dark Current (E_t = 20V) Initial	Final	Signal Current (E_t = 20V, Ill. = 1 fc) Initial	Final	Resolution (E_t = 20V, IS = 200 uA) Initial	Final	Residual Signal (at third scan, E_t = 20V) Initial	Final	Grey-Scale Initial	Final	Gamma Initial	Final
23	2.5 nA		428 nA		525 lines		86%		7 steps		.67	
24	1.3	1.0 nA	224	410 nA	450	300 lines	78(30V)	84%	8	8 steps	.71	.62
25	<0.1	<1	240	395	500	350	78(30V)	80	7	9	.64	.60
26	<1	1.9	240	367	600	400	83	87	10	10	.59	.64
27	1.3		260		650		87		10		.62	
28	5.0	16.0	445	620	600	400	82	80	10	10	.70	.72
29	3.4	9.0	380	500	600	375	84	80	10	10	.66	.68
30	2.3	11.6	413	510	550	500	84		10	10	.67	.65
31	4.6	4.4	237	360	300	525	82		10	10	.70	.66
32	3.0	2.9	290	318	550	500	79		10	10	.69	.64
33	3.5	7.0	370	423	500	600	80		10	10	.67	.66
34	3.0	6.2	415	400	600	600	80		10	10	.69	.67
35	4.3	9.0	355	500	525	450			10	10	.63	.71
36	3.0	6.7	385	442	550	550			10	9	.69	.66
37	3.0	7.0	385	500	500	450			10	10	.71	.73
38	8.5	20.8		559	400	500			8	10	.61	.66
39	8.6	21.4	475	565	525	550			10	10	.67	.65
40	9.0	6.4	390	412	50	600			5	10	.65	.71
41	5.0	5.6	375	422	400	500			10	9	.70	.64
42	5.0	6.6	435	765	350	500			10	10	.69	.66
43	4.0	9.0	475	560	550	550			10	10	.68	.68
44	8.5	15.0	540	489	450	325			10	10	.62	.67

Table I (Cont'd.)

N_G	Dark Current (E_t = 20V) Initial	Dark Current (E_t = 20V) Final	Signal Current (E_t = 20V, Ill. = 1 fc) Initial	Signal Current (E_t = 20V, Ill. = 1 fc) Final	Resolution (E_t = 20V, I_S = 200 uA) Initial	Resolution (E_t = 20V, I_S = 200 uA) Final	Residual Signal (at third scan, E_t = 20V) Initial	Residual Signal (at third scan, E_t = 20V) Final	Grey-Scale Initial	Grey-Scale Final	Gamma Initial	Gamma Final
45	6.8 nA	12.4 nA	423 nA	508 nA	400 lines	325 lines			9 steps	10 steps	.61	.69
46	5.4	7.8	443	426	550	525			10	10	.72	.71
47	5.1		410		475				10		.71	
48	8.1	6.5	486	557	575	600			10	10	.69	.73
49	18.1	38.1	519	698	300	200			7	9	.69	.69
50	17.5	30.2	594	747	450	325			10	9	.64	.67
51	6.2	10.0	378	501	600	475			10	10	.63	.70

Table II

Distribution of 45 Tubes in Terms of Dark-Current Ratio

Dark Current After Sterilization / Initial Dark Current	Number of Tubes E_t = 20V	Number of Tubes E_t = 30V
0.7	1	0
0.8	2	2
0.9	2	0
1.0	3	1
1.1	2	1
1.2	1	1
1.3	3	1
1.4	4	2
1.5	3	2
1.6	1	6
1.7	3	5
1.8	2	1
1.9	0	3
2.0	1	4
2.1	3	3
2.2	2	1
2.3	2	2
2.4	1	1
2.5	2	2
2.6	1	0
2.7	0	0
2.8	0	0
2.9	0	1
3.0	0	0
3.1	0	0
3.2	1	0
3.3	0	1
3.4	0	0
3.5	0	1
3.6	1	0
3.7	0	0
3.8	0	0
3.9	0	1
4.0	1	0
4.8	1	0
5.0	1	0
5.1	0	1
5.2	1	0
6.1	0	2

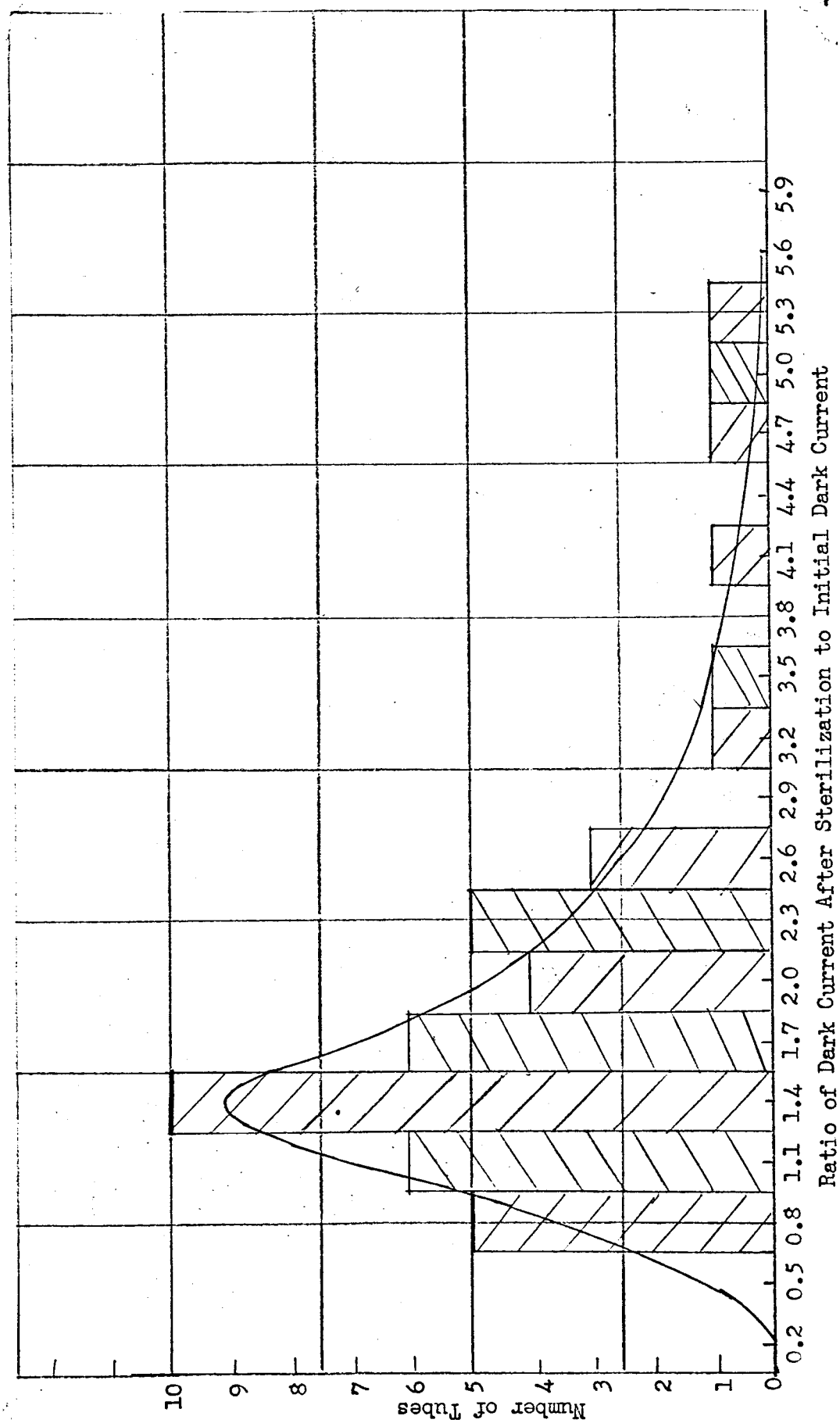

Figure 1. Distribution of Tubes in Terms of Dark Current After Sterilization to Initial Dark Current. Target Voltage = 20 v.

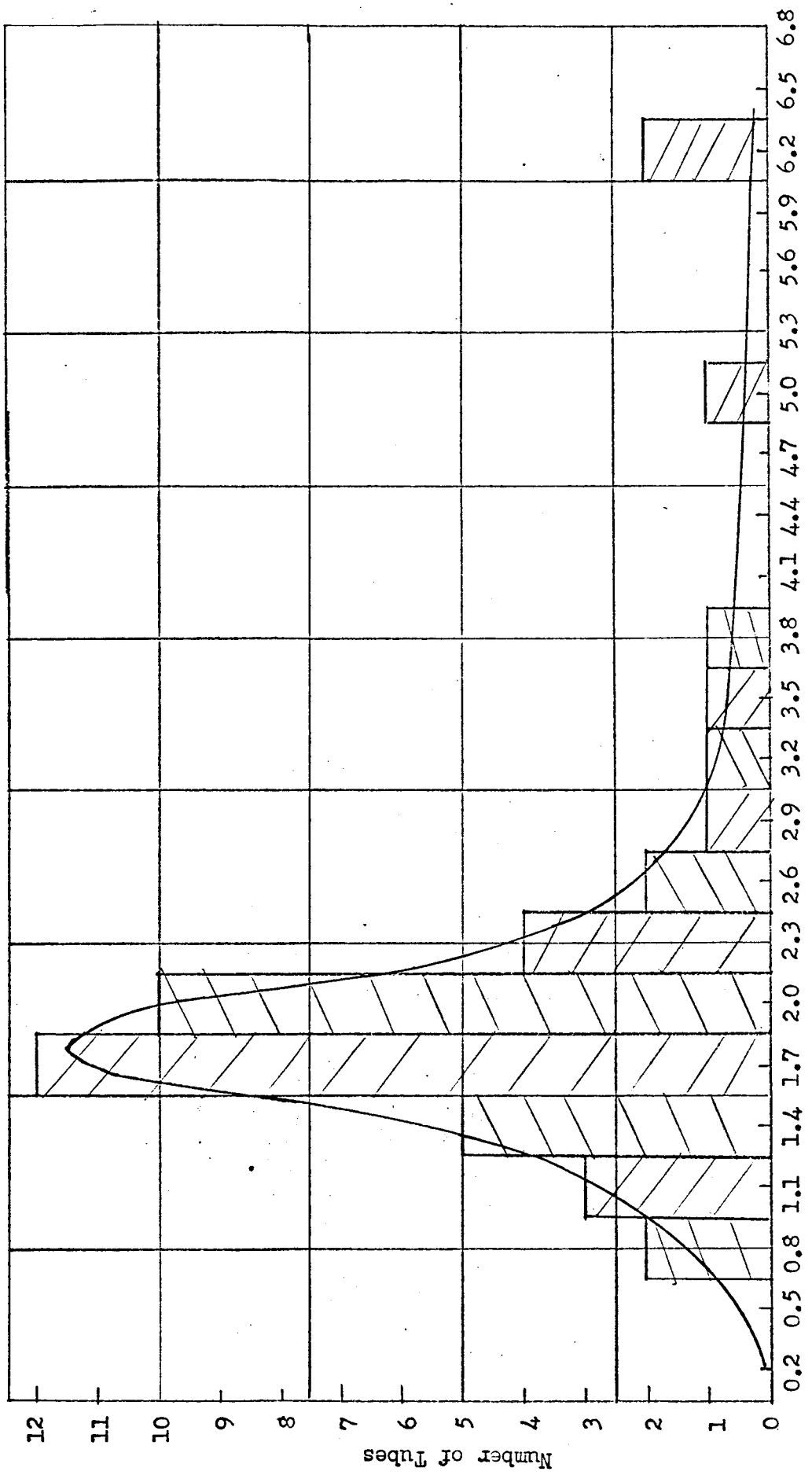

Figure 2. Distribution of Tubes in Terms of Dark Current After Sterilization to Initial Dark Current. Target Voltage= 30 v.

It is seen that at a target voltage of 20V the most probable value of the dark current ratio was in the range 1.40 ± 0.15. However, more than half of the tubes had a ratio higher than this value. The mean value of the ratio was 1.65. Sixty percent of the tubes had a ratio of 2.0 or less, 85% a ratio of 2.5 or less.

For a target voltage of 30V, the most probable value of the dark current ratio was 1.80 ± 0.15, while the mean value was 1.85. Sixty-five percent of the tubes had a ratio of or below 2.0, 85% a ratio of or below 2.5.

The above results are complicated by the temperature dependence of the dark current. It was found that variations in dark current due to changes in the faceplate temperature can be comparable to the changes caused by the sterilization bakes. Therefore, attempts were made in most tests to keep the faceplates at the same temperature for all measurements. The temperature was measured with a thermocouple mounted against the front surface of the faceplate. A flow of cooled air was passed over this surface and adjusted so as to keep the temperature at the desired value. However, it often was not feasible to control the temperature to better than one or two degrees C and, in addition, the temperature of the photoconductive layer, on the back side of the faceplate, may have had a significantly different value from that indicated by the thermocouple.

In order to obtain an indication of the significance of variations in temperature, measurements were made of the dark current of some representative tubes at different temperatures. Figure 3 shows the results of such measurements on five tubes, made at a target voltage of 20V, on a semilog plot. In the case of the 2 tubes where more than two measurements were obtained the uncertainty of the results is clearly seen in the spread of the experimental points. This spread most likely is an indication of the difference between the nominal thermocouple readings and the true photoconductor temperatures. However, there can be little doubt about the sizable rate of rise in dark current with temperature. Most measurements were made at an indicated temperature of between 22°C and 30°C. It can be seen that a variation in temperature of 2°, within this range, can easily account for a dark current change of 20%.

As can be seen from Table I, wide variations existed between the dark current values obtained from different tubes. Little correlation is found between the sensitivity and dark current measurements of any given tube. Therefore, it appears possible that the dark current can be kept small even in tubes of high sensitivity.

In Fig. 4 the dark current characteristics for 3 typical tubes are shown before and after the full sterilization process. The approximate faceplate temperature at which the measurements were made

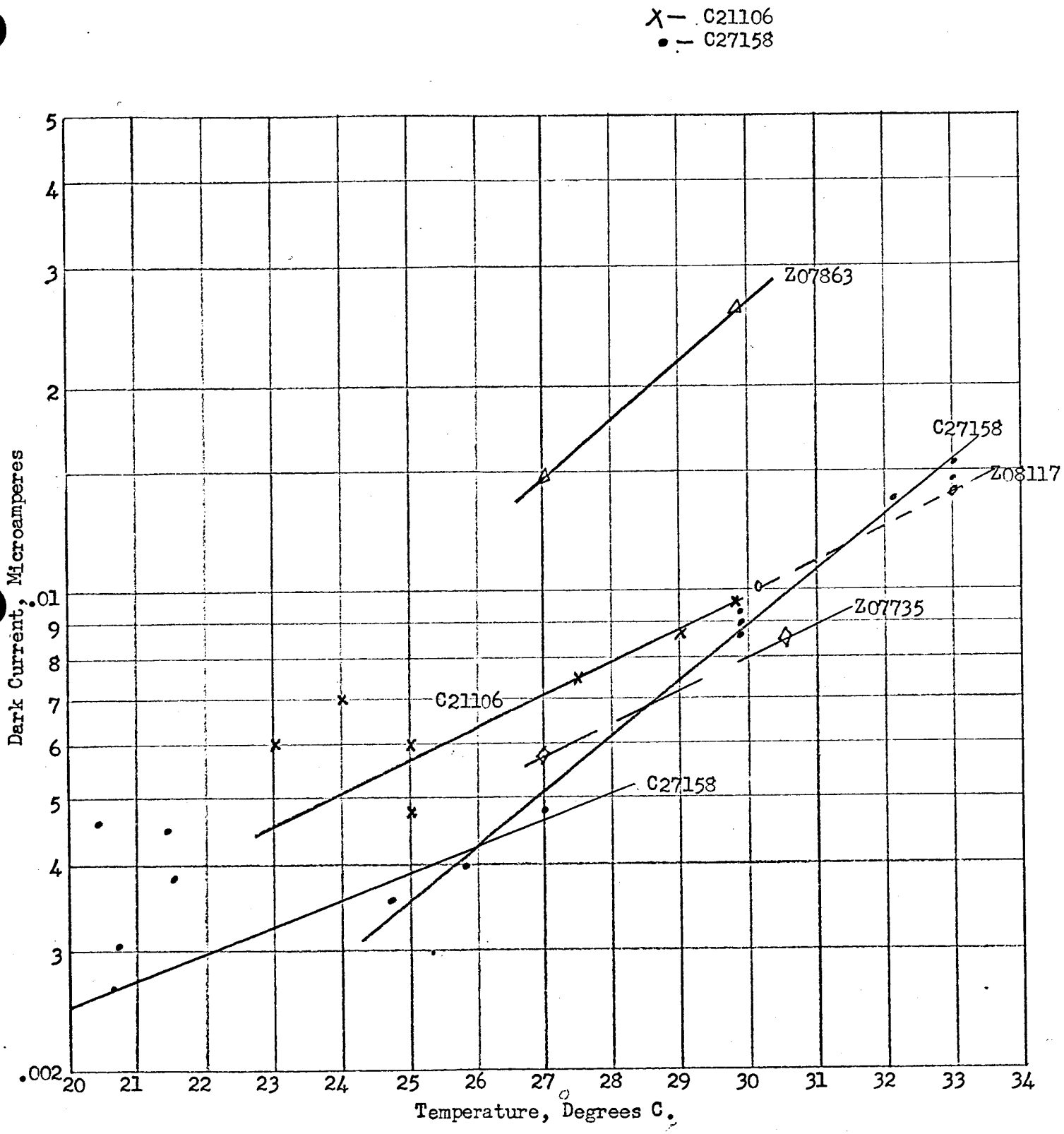

Figure 3. Semilog Plot of Dark Current (of Five Tubes) vs. Temperature. Target Voltage = 20 v.

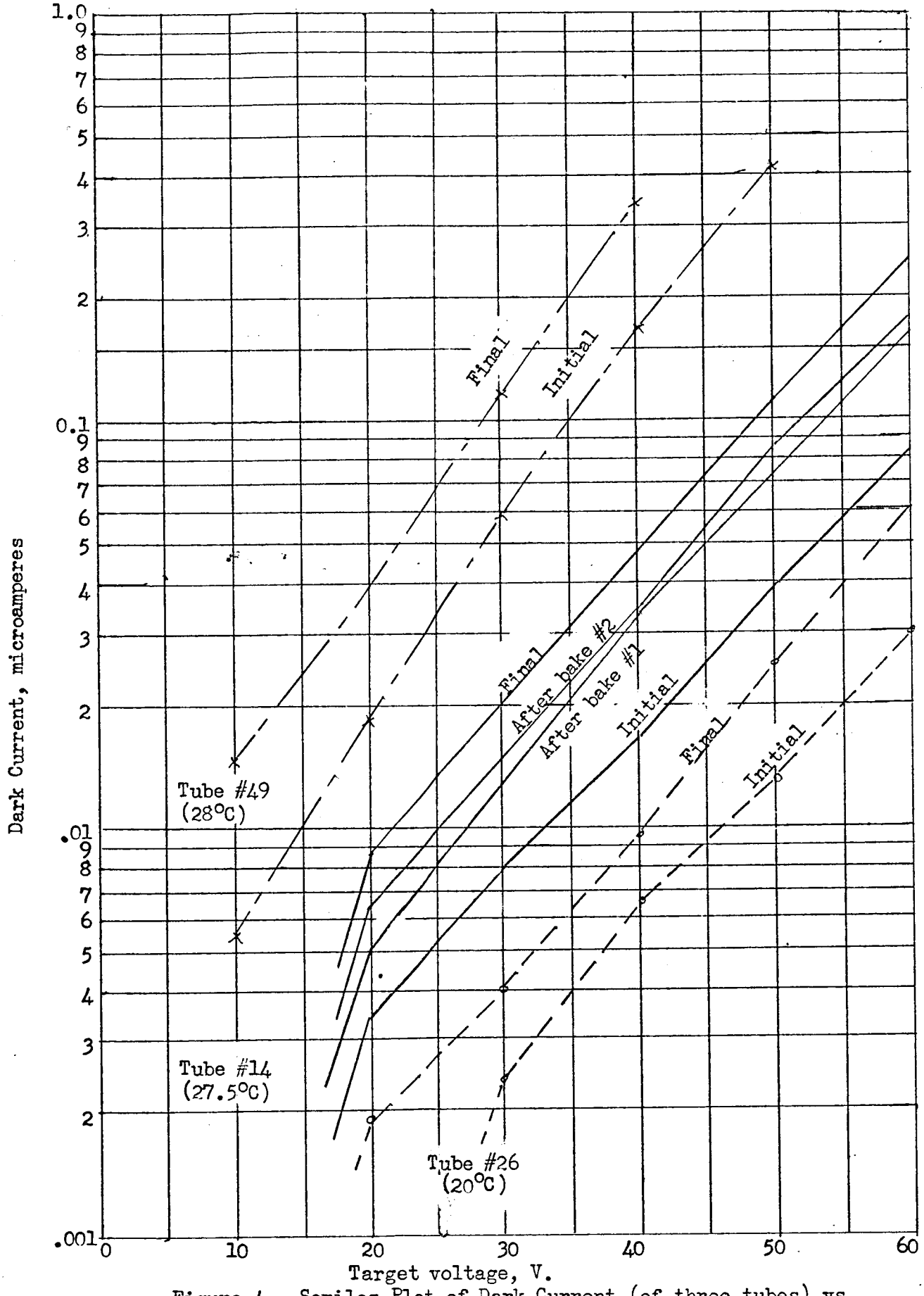

Figure 4. Semilog Plot of Dark Current (of three tubes) vs. Target Voltage, Before and After Dry-Heat Sterilization.

for each tube is indicated. For one tube (#14), the results obtained after the first and second sterilization bakes also are given. In general it was found that the increase in dark current due to the first bake was greater than for the subsequent bakes.

The results reported above suggest that for any given tube it is likely that sterilization will cause an increase in dark current at constant target voltage of less than 100%.

B. Sensitivity

In general, the sensitivity of the photoconductor chosen for this project was found to increase as a result of the dry-heat sterilization, but by a smaller percentage than the dark current. Figure 5 is a graphical presentation of the distribution of 44 vidicons as to change in signal current at 20V target voltage, for uniform illumination of one footcandle intensity. The most probable ratio of sensitivity after sterilization, to initial sensitivity, as well as the mean value of this ratio, according to these results is about 1.25.

Although temperature changes of the faceplate caused some corresponding variations in signal current, these represented a much smaller percentage change than the corresponding effect with dark current. In the case of one tube in which the faceplate temperature was changed from 23°C to 30°C, at one footcandle illumination and 20V target voltage, the signal current rose by less than 10%.

Typical plots of signal current vs. target voltage at 1.0 fc faceplate illumination are given in Fig. 6 for two experimental tubes. As was found in the case of dark current, the increase in sensitivity after the first bake was greater than after the second and third.

The measurements indicated that the sensitivity of any future tube with the photoconductor used in this project, can be expected to increase by about 25% during sterilization.

C. Light Transfer Characteristic

The log-log plots of signal current vs. target illumination for the various tubes in most measurements were slightly concave upward, i.e. the slope of the curves was lower at smaller light levels. The gamma values given in Table I are the average slopes of the various curves. In Fig. 7 the distribution of tubes in terms of gamma is shown, before and after sterilization. The average values of gamma for the two sets of measurements are the same within the accuracy of the data. The difference in shape of the two distribution graphs also is within the expected uncertainty of the measurements. It can, there-

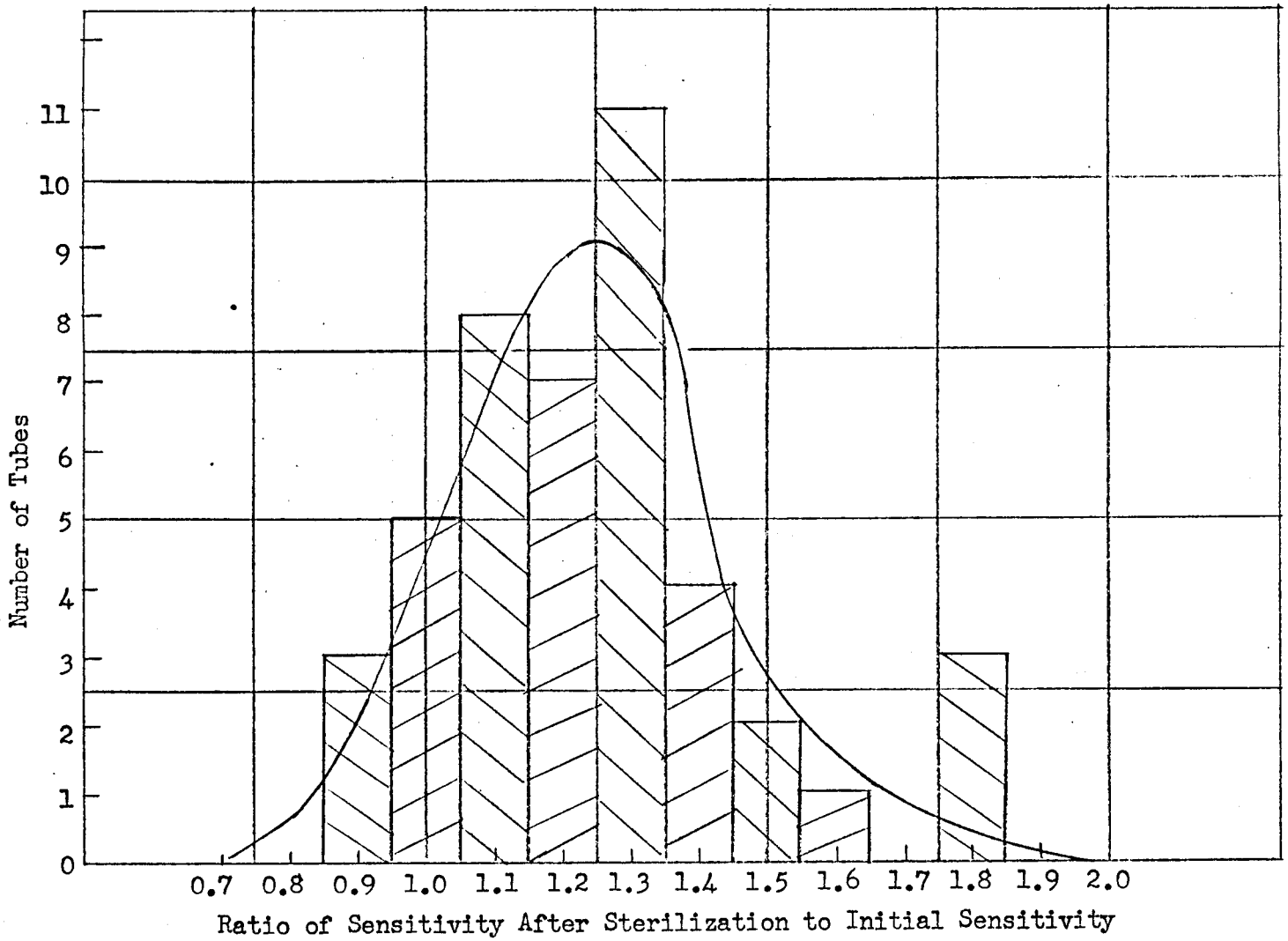

Figure 5. Distribution of Tubes in Terms of Sensitivity (Signal Current at 1.0 ft-cd Target Illumination) After Sterilization to Initial Sensitivity. Target Voltage = 20 v.

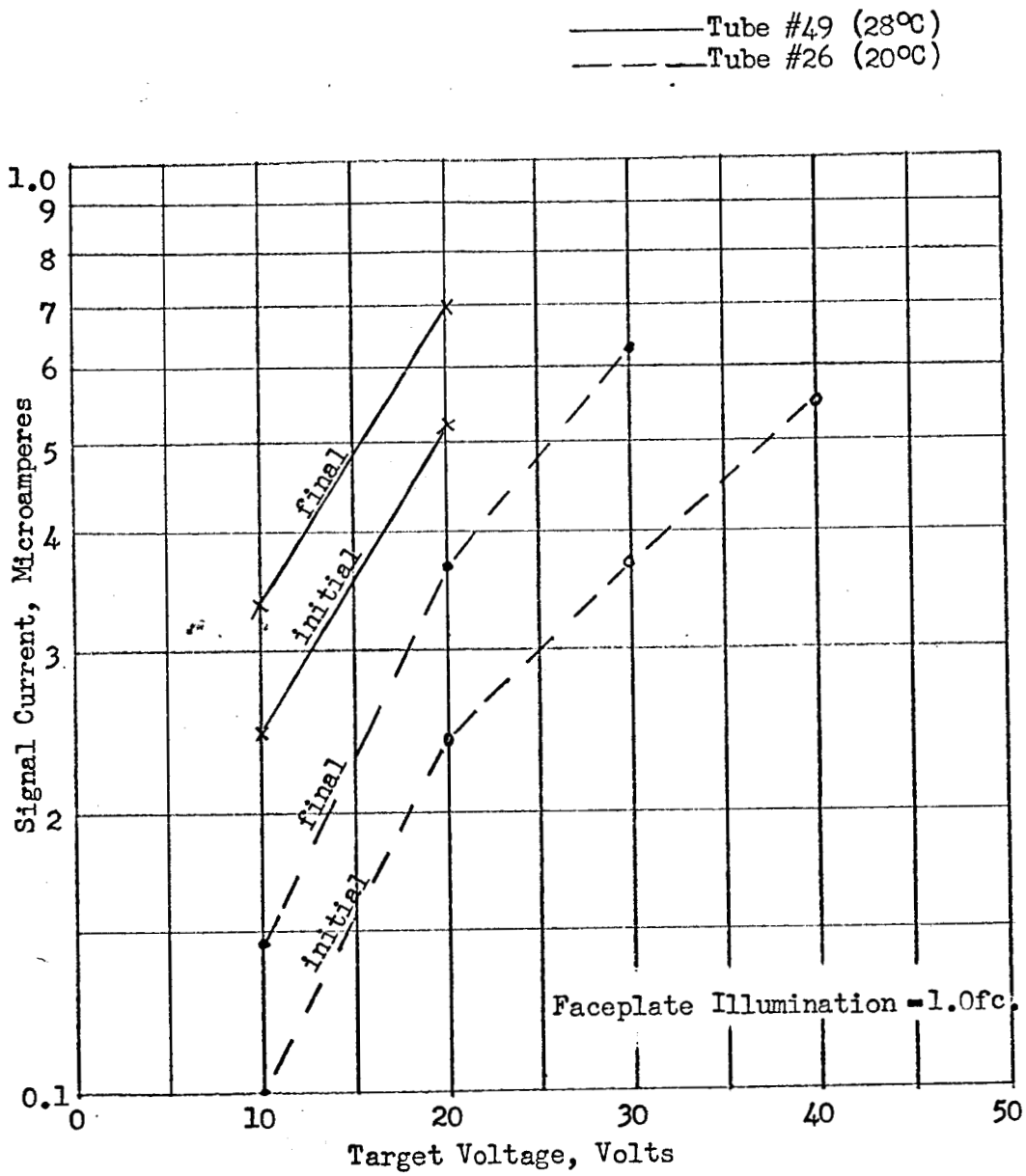

Figure 6. Semilog Plot (for Two Tubes) of Signal Current at 1.0 ft-cd Target Illumination vs. Target Voltage.

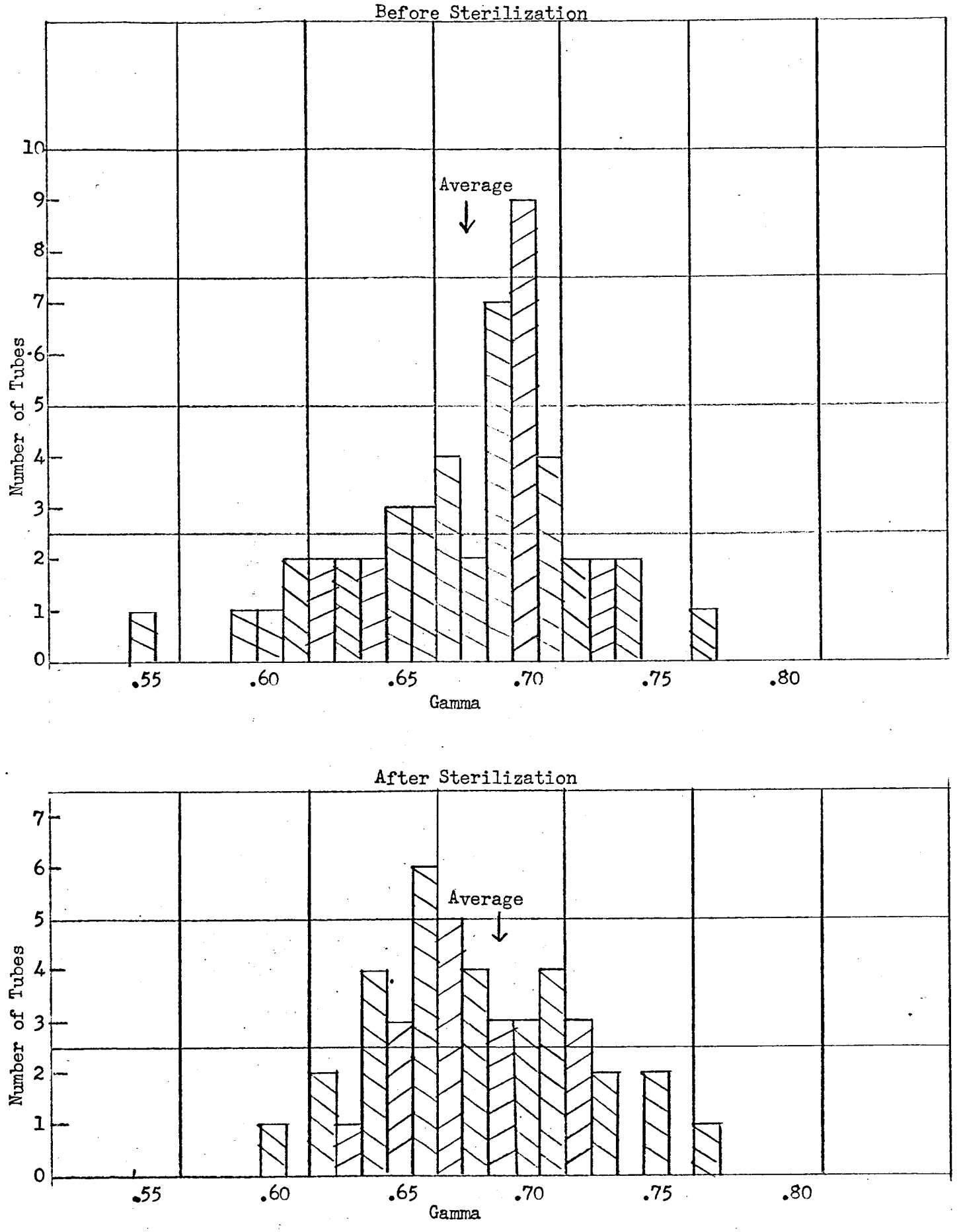

Figure 7. Distribution of Tubes, Before and After Sterilization, in Terms of Gamma. Target Voltage = 20V.

fore, be concluded that the light transfer characteristic of the experimental photoconductor is not sensitive to the sterilization process as far as shape and slope of the curve are concerned. The gamma of the photoconductor generally falls in the range of 0.68 ± 0.04.

A set of measurements were made on one tube (No. 22) when scanned with a one-second frame time. The data were taken before the tube was dry-heat sterilized. Unfortunately, the tube was lost when the oven overheated during the third sterilization bake causing failure of the indium seal, at the faceplate. Due to time limitations, no other such slow-scan measurements were made on later tubes.

The data obtained from tube No. 22 are shown in Fig. 8. The measurements were made at various exposure times ranging from 0.01 sec. to 0.5 sec. The straight line drawn so as to average the experimental points corresponds to a gamma of 0.71. The value of gamma measured for this tube at standard television rate was 0.68. It is seen that a measurable signal was obtained below an exposure of 0.002 ft.-cd.-sec. and that saturation appears to set in somewhat above 0.15 ft.-cd.-sec.

D. Spectral Response

Figure 9 shows the average spectral response of eleven tubes before and after sterilization. Measurements were made at six wavelengths ranging from 500 to 666 millimicrons. The experimental results for each tube were adjusted so that the values quoted correspond to the same amount of power at all wavelengths incident on the faceplate. The curves for the different tubes were then normalized to the same maximum response value, which in all cases occurred at the 566 mu reading. The two curves in Fig. 9 represent the average of these normalized response characteristics. It is seen that after sterilization the response at wavelengths above and below the peak of the curve has somewhat increased relative to the peak response, i.e. the curve has become slightly flatter.

Data taken on four earlier tubes, made before the slight modification in the photoconductor, showed less consistent results than the eleven tubes mentioned above which were made with the later form of photoconductor. The maximum response for the four earlier tubes occurred at somewhat shorter wavelengths (at or below 500 mu) than for the later tubes.

E. Resolution

The distribution of tubes, before and after sterilization, in terms of ultimate resolution is shown in Fig. 10. The average resolution was found to have decreased from an initial value of 500 lines to a final value of 460 lines. Of the forty-four tubes tested for resolution before and after full sterilization: twenty-seven tubes decreased in resolution,

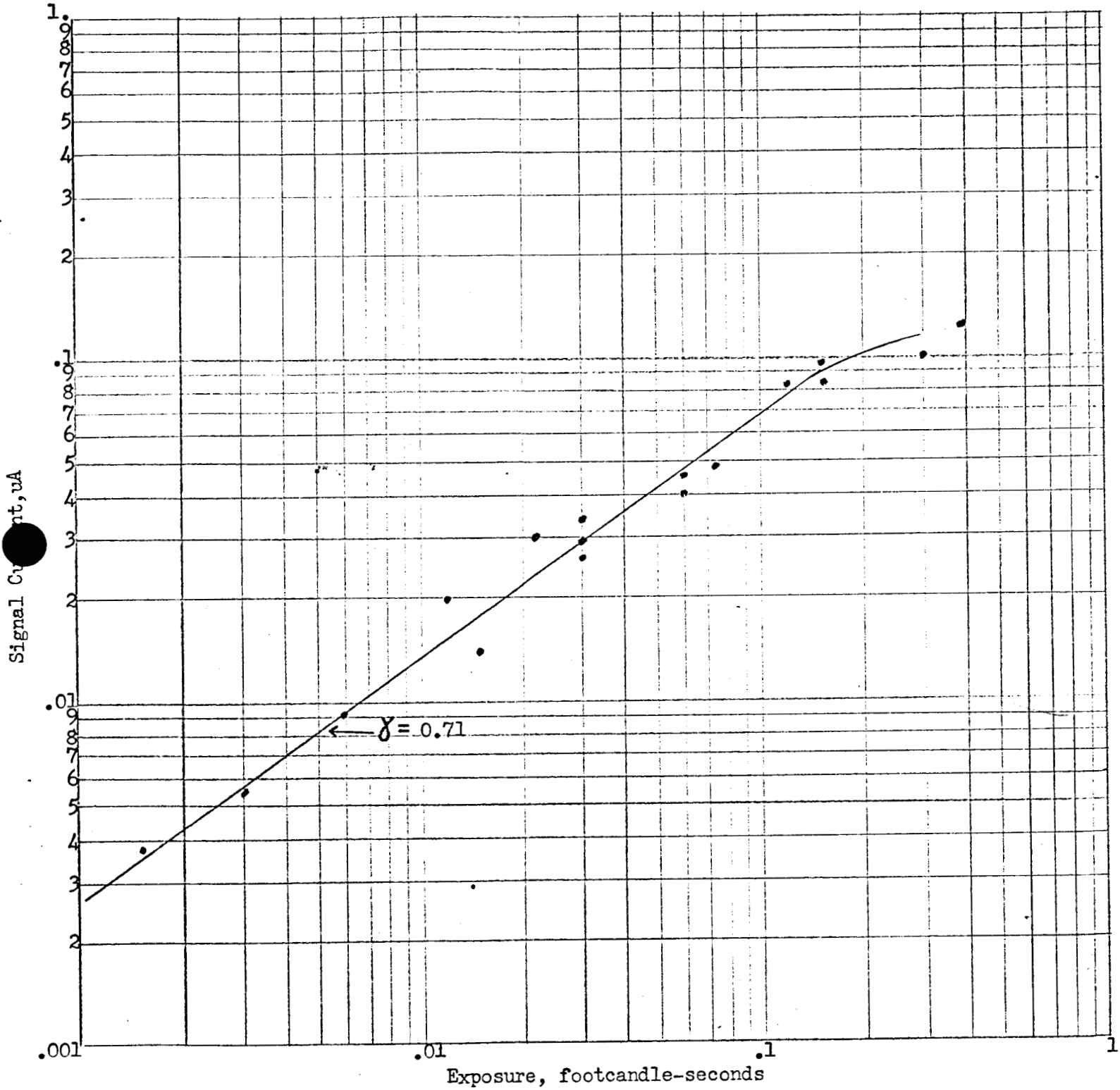

Figure 8. Light Transfer Curve of Tube No. 22 at Slow-Scan Rate. Frame Time = 1 second. Target Voltage = (26 ± 1)V.

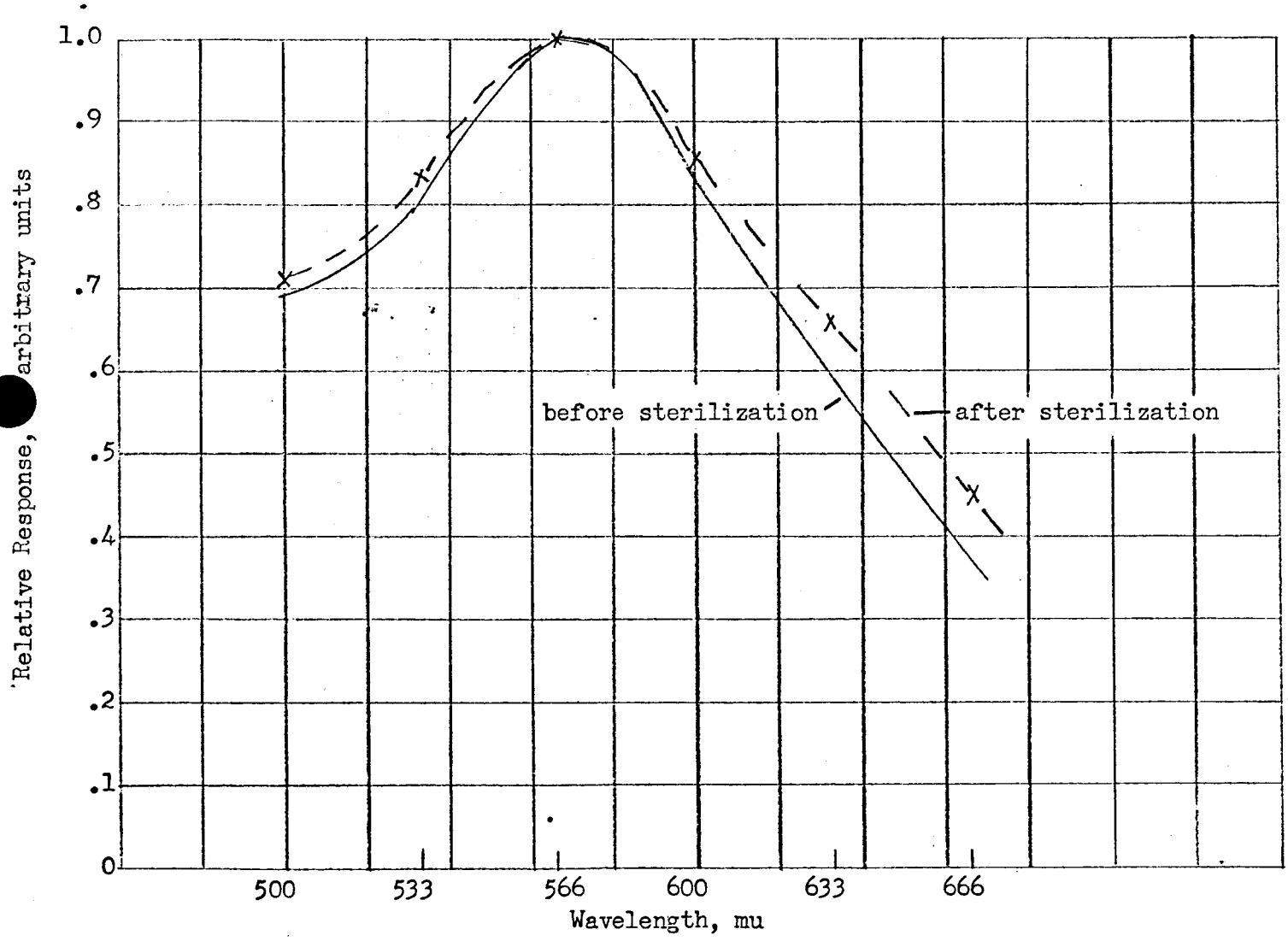

Figure 9. Average Spectral Response (of 11 tubes) Before and After Sterilization. Target Voltage = 20 V.

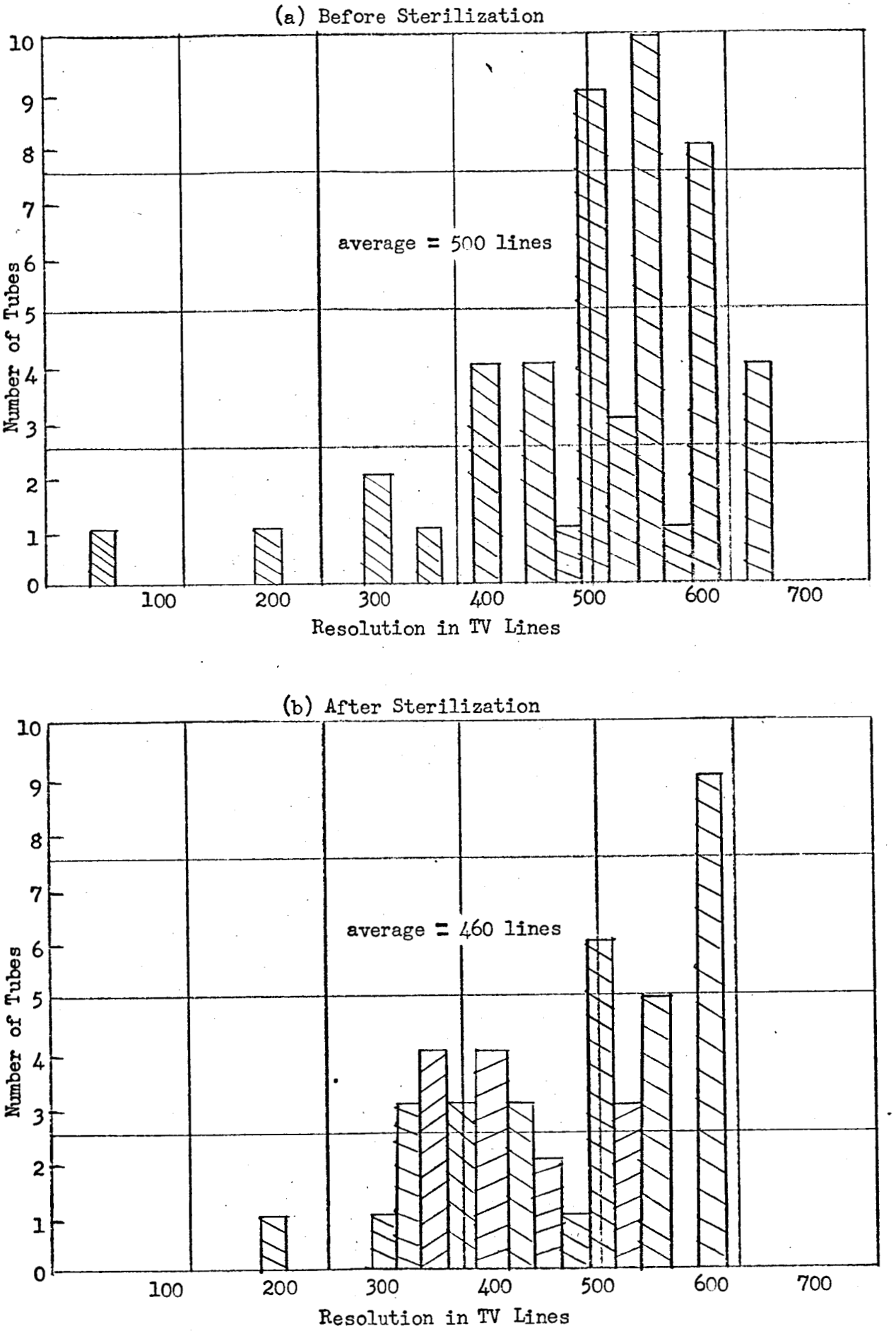

Figure 10. Distribution of Tubes, Before and After Sterilization, in Terms of Resolution. Target Voltage = 20 v., Signal Current = 0.2 ua.

five remained unchanged, and twelve increased during sterilization. It therefore appears that the exposure of the experimental photoconductor to three dry-heat sterilization cycles can be expected to result in a small deterioration of its resolution capability.

F. Gray-scale

In Fig. 11 the distribution of vidicons is shown, before and after sterilization, as to gray-scale rendition. It can be seen that three-quarters of each set of tubes could distinguish the full ten gray-scale steps. The average number of gray-scale steps was essentially the same, 9-1/4 before and 9-1/2 after sterilization.

The gray-scale pattern used for this measurement was limited to ten steps. It is likely that some of the tubes would have been capable of distinguishing a larger number of steps.

G. Erasure

The residual signal, at the third scan after removal of the illumination, was measured on 33 tubes before sterilization and on 15 tubes after sterilization. No significant change was observed. As indicated in Fig. 12, the average residual signal in either case was 80-1/2% of the original signal.

V. DISCUSSION

The aim of Task I was to develop and demonstrate a photoconductor suitable for slow-scan operation and able to survive the necessary sterilization requirements.

Work performed in preparation for this contract already had indicated that an ASOS photosurface with rhodium signal plate on a high-quality quartz substrate is relatively immune to the dry-heat sterilization process.

Fifty-one tubes were made using the ASOS photosurface. Forty-five of these tubes were exposed to the full set of three 36-hour 145°C sterilization bakes. The remaining six tubes were lost, due to various incidental circumstances not connected with the behavior of the photoconductor.

Three tubes were also exposed to the ethylene-oxide decontamination process without any appreciable effect.

The effect of the sterilization bakes consisted primarily of an increase in dark-current and a smaller rise in sensitivity. The data indicates that the dark current can be expected to grow by less than 100% and the sensitivity by about 25%. These changes are well within the range of these quantities as found in different tubes and it is felt that they are highly acceptable.

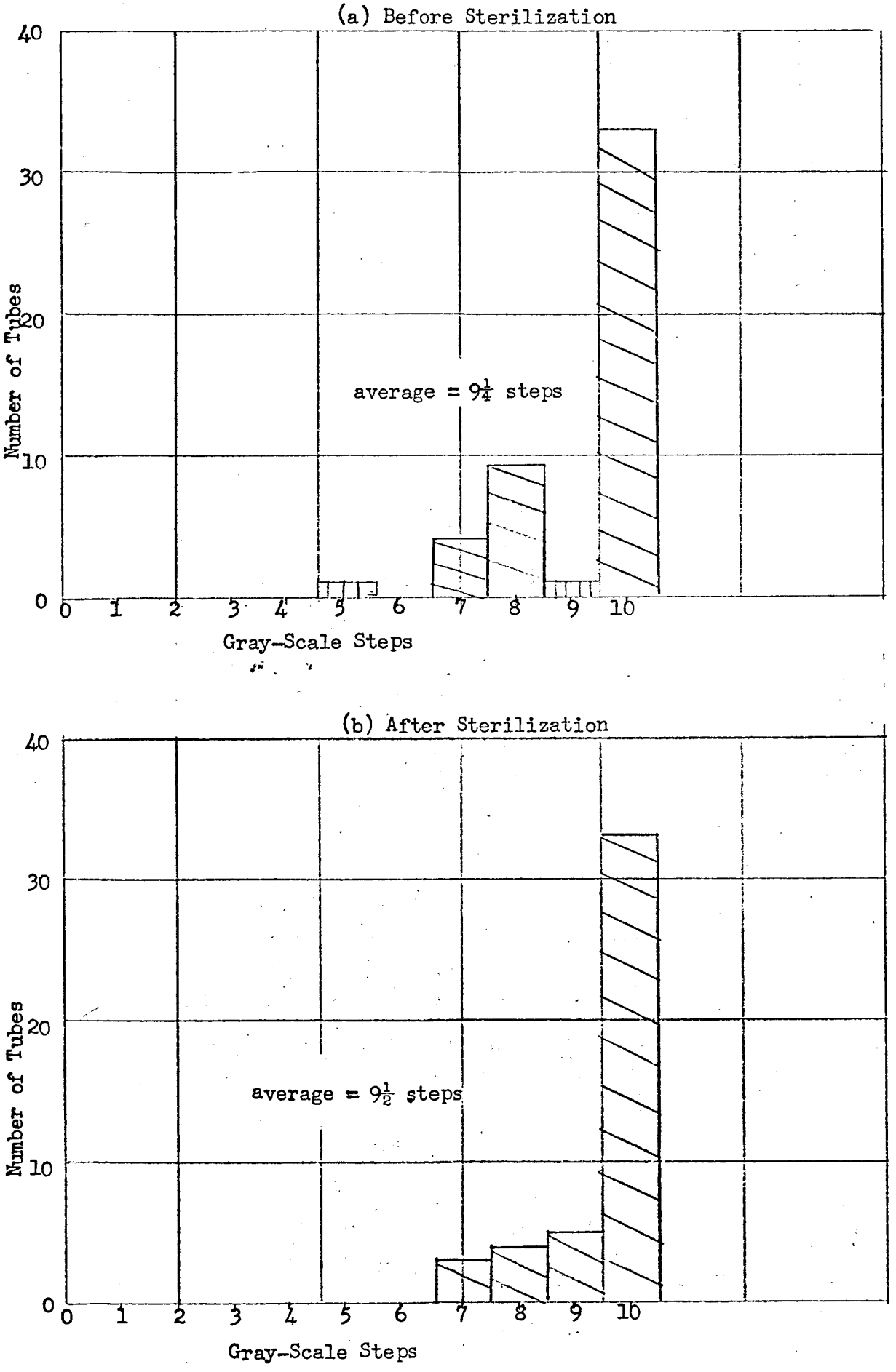

Figure 11. Distribution of Tubes, Before and After Sterilization, in Terms of Gray-Scale Rendition. Target Voltage = 20 v.

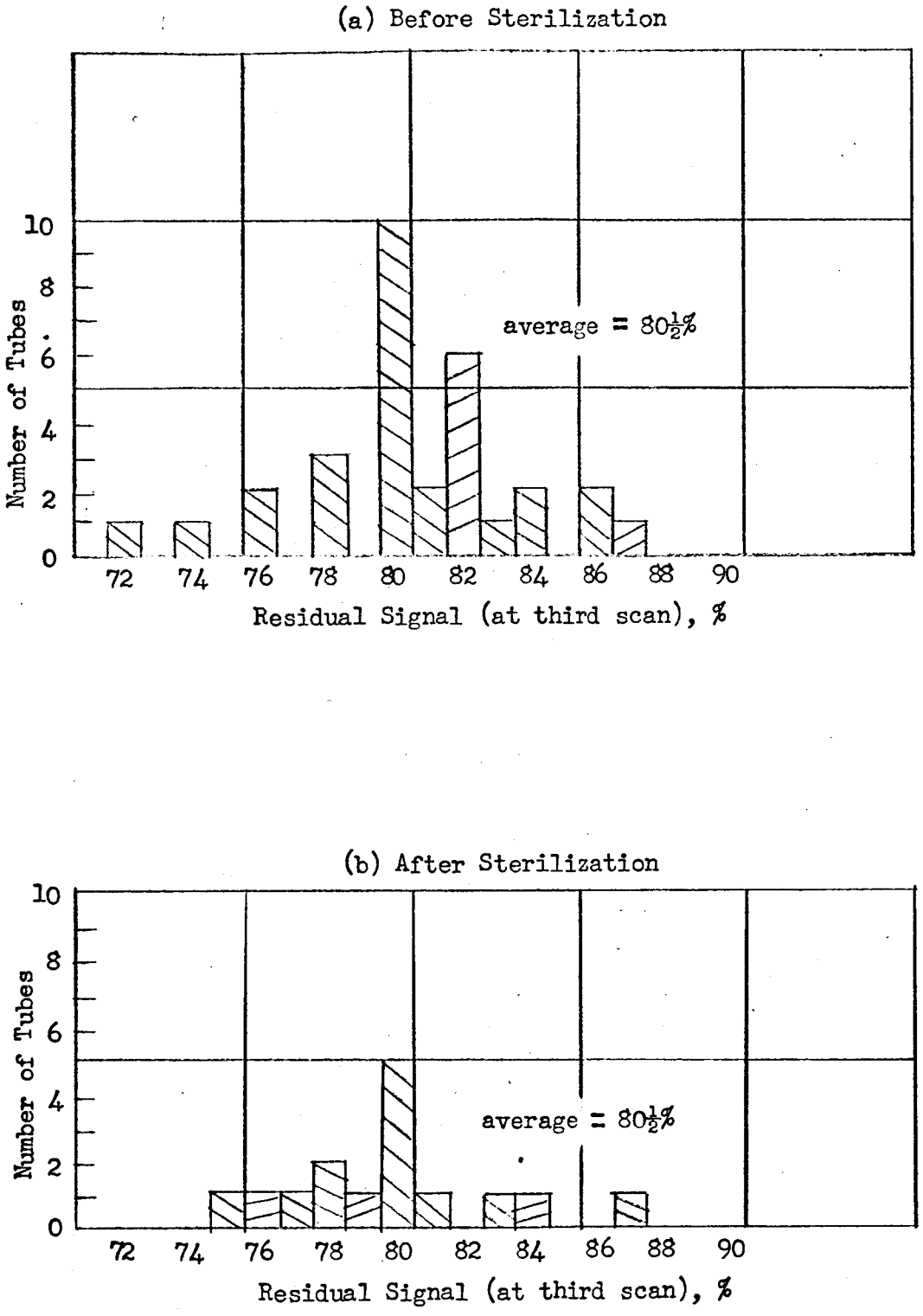

Figure 12. Distribution of Tubes, Before and After Sterilization, in Terms of Residual Signal at Third Scan after Removal of Light. Target Voltage = 20 V., Original Signal Current = 0.2 ua.

In addition a small deterioration in resolution and, possibly, a minor shift in the spectral response toward longer wavelengths were observed. No systematic changes were found in gamma, gray-scale rendition or lag.

The measurements made during Task I were necessarily limited in scope. The chief emphasis was not so much on ascertaining the precise characteristics of the photoconductor under study, as it was on testing its stability under sterilization and decontamination procedures.

Practically no work was done at slow-scan rates, although the photoconductor is intended to be used under such conditions. Both the greater availability of standard-rate equipment and the considerable time-saving in testing at faster rates, made it impractical to do this work at less than sixty fields per second. There is no reason to believe that the effect of the sterilization bakes is any different at slower scan rates than it is at the standard television rate.

As a final presentation of the results obtained on Task I, Fig. 13 shows the average performance of all the tubes which were tested before and after the complete sterilization procedure. Dark current and signal current (at one-footcandle faceplate illumination) are shown as a function of target voltage. These curves can serve as a guide in predicting the behavior of a photosurface made in the manner of those described in this report.

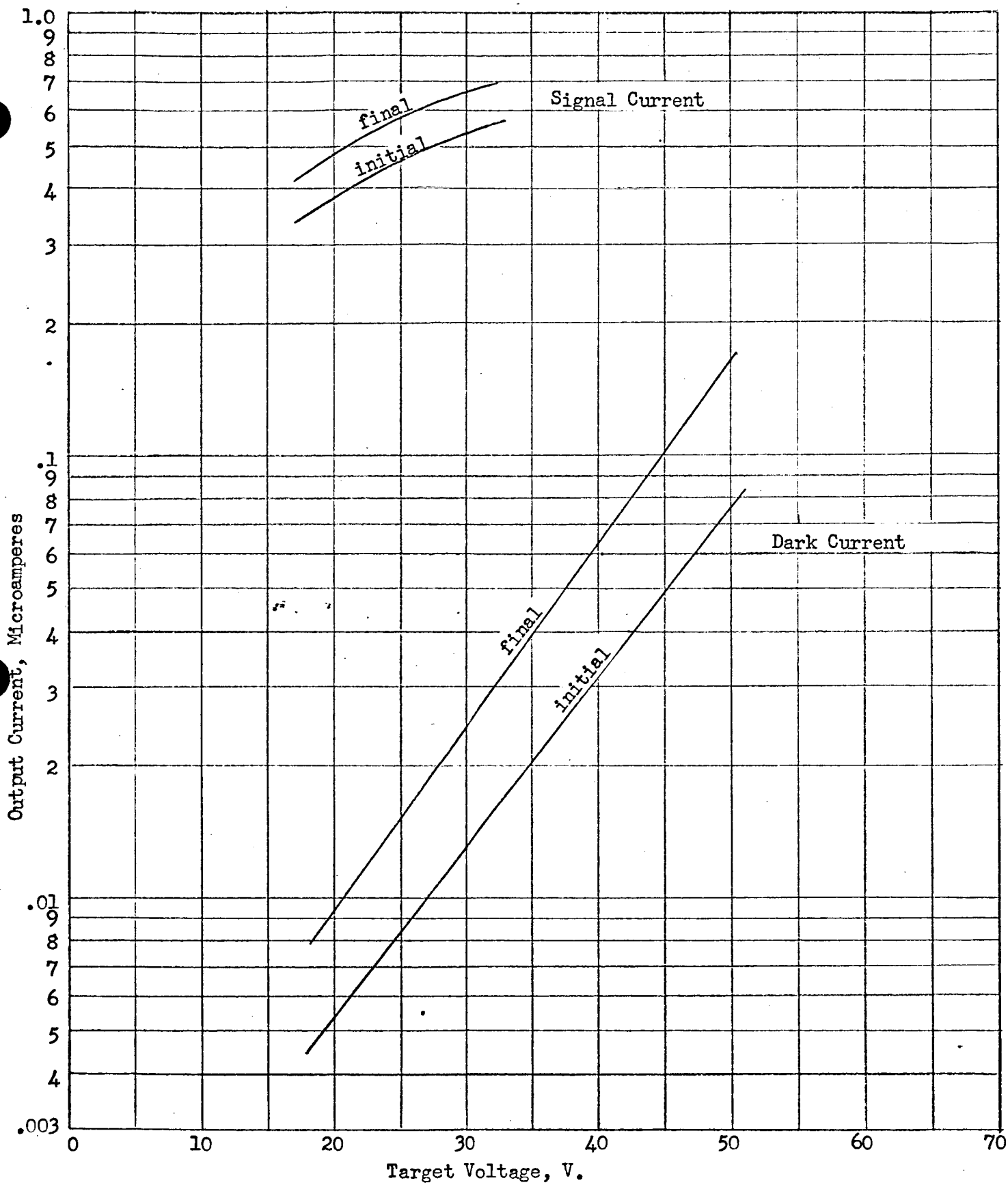

Figure 13. Semilog Plot of Average Dark Current and Average Signal Current at 1.0 ft-cd Faceplate Illumination vs. Target Voltage, Before and After Sterilization. Number of Tubes Included for Dark Current = 45, for Signal Current = 20.

I. DESIGN

The camera tube developed under this contract is an electrostatically focused and deflected 1" vidicon. In electrical design it is similar to several commercial tube types. Its outstanding characteristic is its extreme ruggedness. In order to meet the required specifications, a novel approach had to be taken to the physical design of the tube, for the enclosure as well as the internal elements.

Four basic requirements guided the design:

(a) All structural features had to be able to withstand the required sterilization and environmental tests.

(b) The cathode surface and the photoconductor could not be exposed to brazing temperatures.

(c) The tube should have no magnetic materials, except in the bottom section.

(d) Only a limited time (about five months) was available for designing and procuring all components, jigs and fixtures needed for starting tube construction.

The basic design achieved during this contract period is depicted in Fig. 14, while Fig. 15 shows a photograph of an actual, unpotted tube.

As a means of ruggedization, the entire structure was designed to consist of brazed ceramic and metal components. The only exception is the quartz faceplate which is attached by an indium seal. Strength tests on faceplate subassemblies showed that this sealing method is satisfactory.

The lens and deflectron electrodes were designed to be made of evaporated copper, possibly covered with electroplated gold. Such electrodes were found capable of withstanding the brazing operations. Other internal electrodes consist of preformed metal parts.

In order to provide electrical connections to the inside of the tube, molybdenum pins were designed which are brazed into the ceramic tube wall. Leads are attached to the outside end of each pin by soldering or welding.

External View (Without Potting or Shielding)

Cross Sectional View

All dimensions are in inches

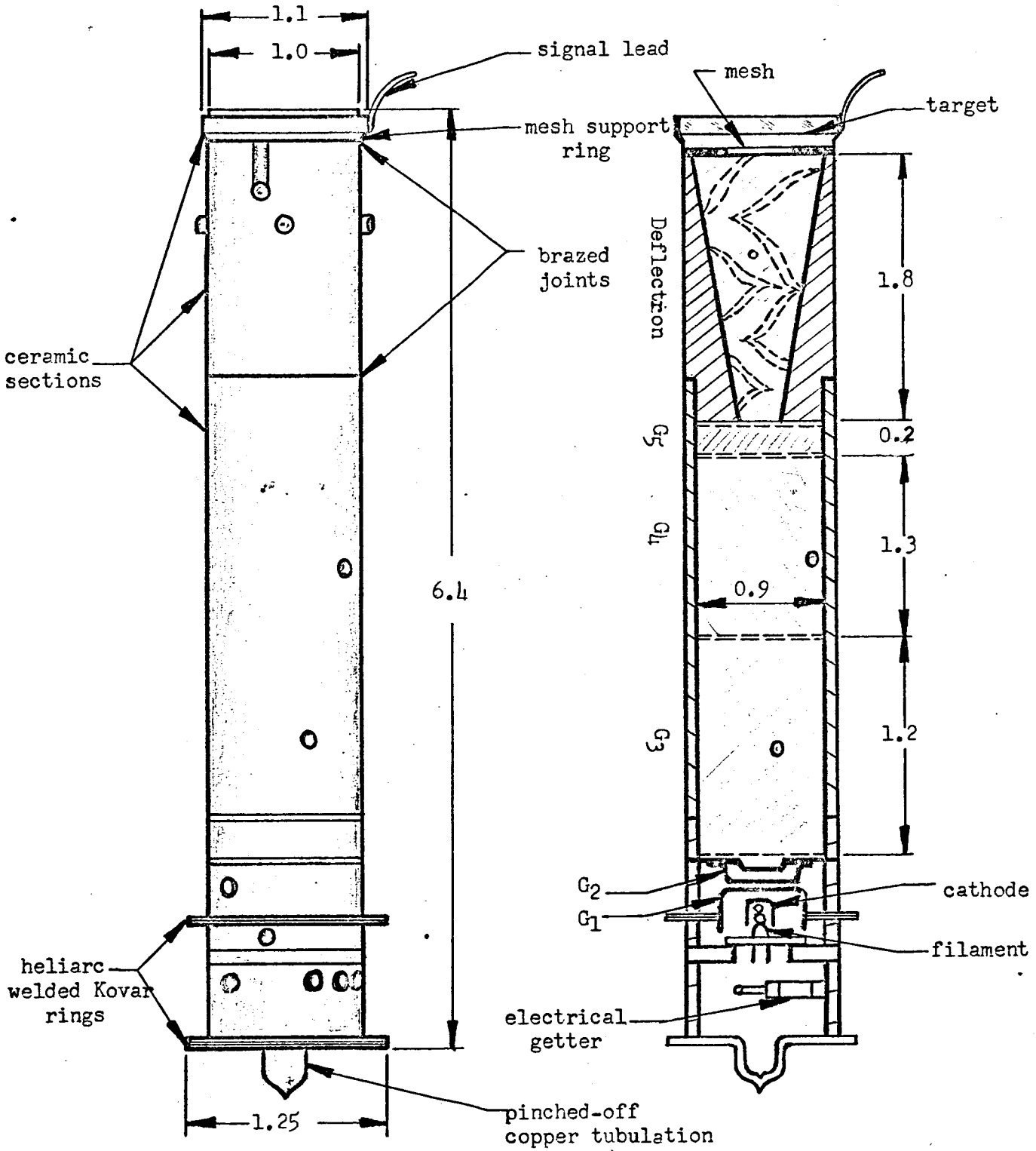

Fig. 14. External and Cross Sectional View of Complete (Unpotted) Ceramic Vidicon

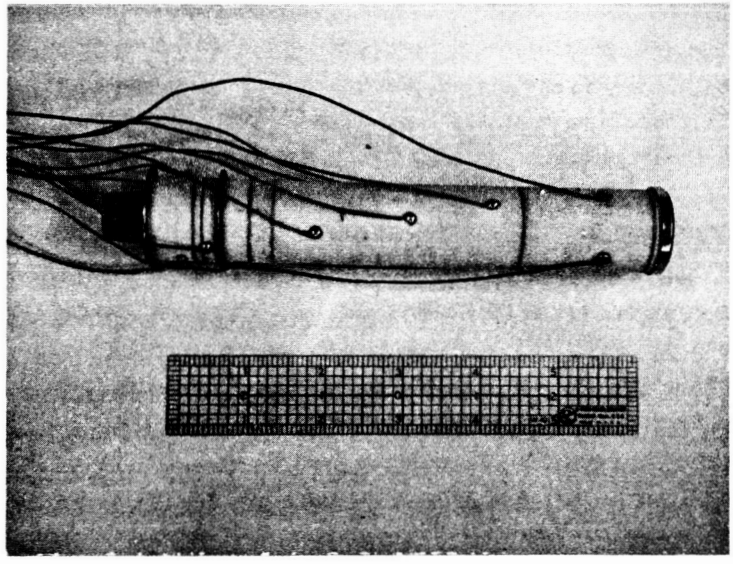

Fig. 15. Ceramic Vidicon

Several electrical connections are made via the brazed joints which hold the various tube components together.

Brazing jigs were developed which ensure good alignment of the various tube components as well as reliable brazed joints. Similarly, jigs were designed for holding and cooling the Kovar flanges during the heliarc welding operations, and optimum welding parameters were determined.

Work done prior to this contract indicated that mechanically tensioned (rather than fired) nickel mesh has the highest resistance to damage under exposure of shock of all available mesh materials. Further tests, performed under this contract, reaffirmed this fact. The mesh design, therefore, is based on 1000-line (per inch) nickel mesh, mechanically tensioned on a flat nichrome ring which is screw mounted to a support ring. The latter is a molybdenum disk which is part of the stacked ceramic-metal tube body (see Fig. 14).

The three-element electrostatic electron lens and the five-cycle deflectron were designed according to standard procedures, with particular emphasis being given to minimizing lens and deflection aberrations. The deflectron was made a part of the third lens electrode (G_5). Therefore, the center potential of the deflectron nominally should be at the same voltage as G_5.

The deflectron portion of the tube was made a separate ceramic section which forms part of the tube envelope.

It was decided early in the contract that it would be desirable to use the low-power (0.6 watt) "dark heater" gun which had been previously developed by RCA. However, a method had to be found of ruggedizing its construction while maintaining accurate alignment and spacing of its parts. The resultant design is shown in Fig. 16.

Standard parts are used in constructing the gun, but they are mounted in a novel fashion. The G_2 electrode, which consists of several sections, is first welded together with accurate alignment (checked by microscope) of its upper (defining) and lower apertures. The G_2 and G_1 electrodes are then brazed to a ceramic spacer and to the G_2 support ring, thereby becoming an integral part of the tube structure. Good alignment is achieved by using a brazing jig which positions the gun electrodes in their proper location relative to the axis of the tube.

In a subsequent operation, the cathode subassembly is mounted inside the G_1 cup. A precision jig was designed to ensure accurate spacing between

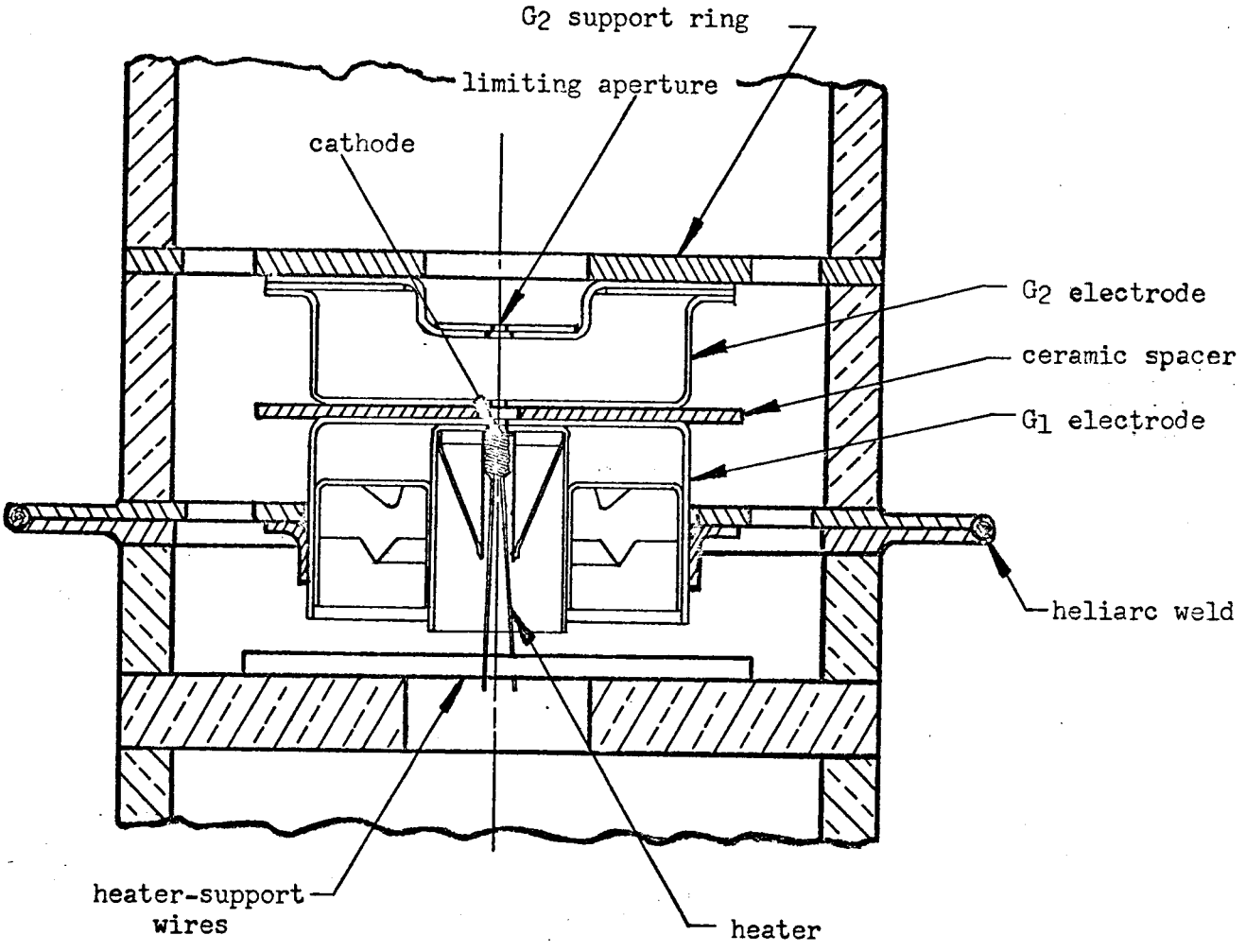

Fig. 16. Cross Sectional View of Gun Section of Ceramic Vidicon

the cathode surface and the G_1 electrode.

The lower section of the tube (less copper tubulation) is then attached by heliarc weld. The lower section provides two Kovar wires to which the heater legs are attached after the heater has been slipped into the cathode sleeve.

The getters chosen for this application are exothermic units flashed by current fed into the tube through the wall pins. It was found that the ceramic tube walls are sufficiently translucent to permit visual monitoring of the flashing operation.

The tube is evacuated through a copper tubulation on a Kovar header which is attached by means of another heliarc weld. After the proper pump-down, bake and cathode activation, the tube is removed from the pump by means of a pinch-off at the copper tubulation.

As a separate project, some work was performed on a ceramic cathode consisting of a directly heated cathode on a ceramic substrate. A typical sample is shown in Fig. 17. The design shown in Fig. 17 should provide greater strength, simpler construction and, possibly, lower power consumption than the present design. In its final form this structure might include the control electrode (G_1) and the accelerator electrode (G_2) as part of the same structure.

Several units of a design similar to that shown in Fig. 17 were made and tested. The heater pattern was formed of molybdenum metalizing applied by a silk screen process. Although the electron emission was low (1.5 mA maximum), the results were encouraging and indicated that the necessary operating temperatures can be reached and that reasonable lifetimes may be obtainable.

Test results on potting compounds indicated that a specific formulation of a polyurethane (PR 1538) is able to withstand the required sterilization treatments and has a sufficiently high stiffness (although a stiffer material would be preferable).

Shielding efficiency and impact tests on shielding materials showed that Moly Permalloy (which had been suggested by JPL) was satisfactory. The appearance and approximate dimensions of the potted tube are indicated in Fig. 18. The total mass of a complete potted tube is about 419 grams including leads with banana plugs. The mass of the potting and shielding materials is about 171 grams.

II. MANUFACTURE OF TUBES

In general terms, the basic steps in the production of a ceramic vidicon are as follows:

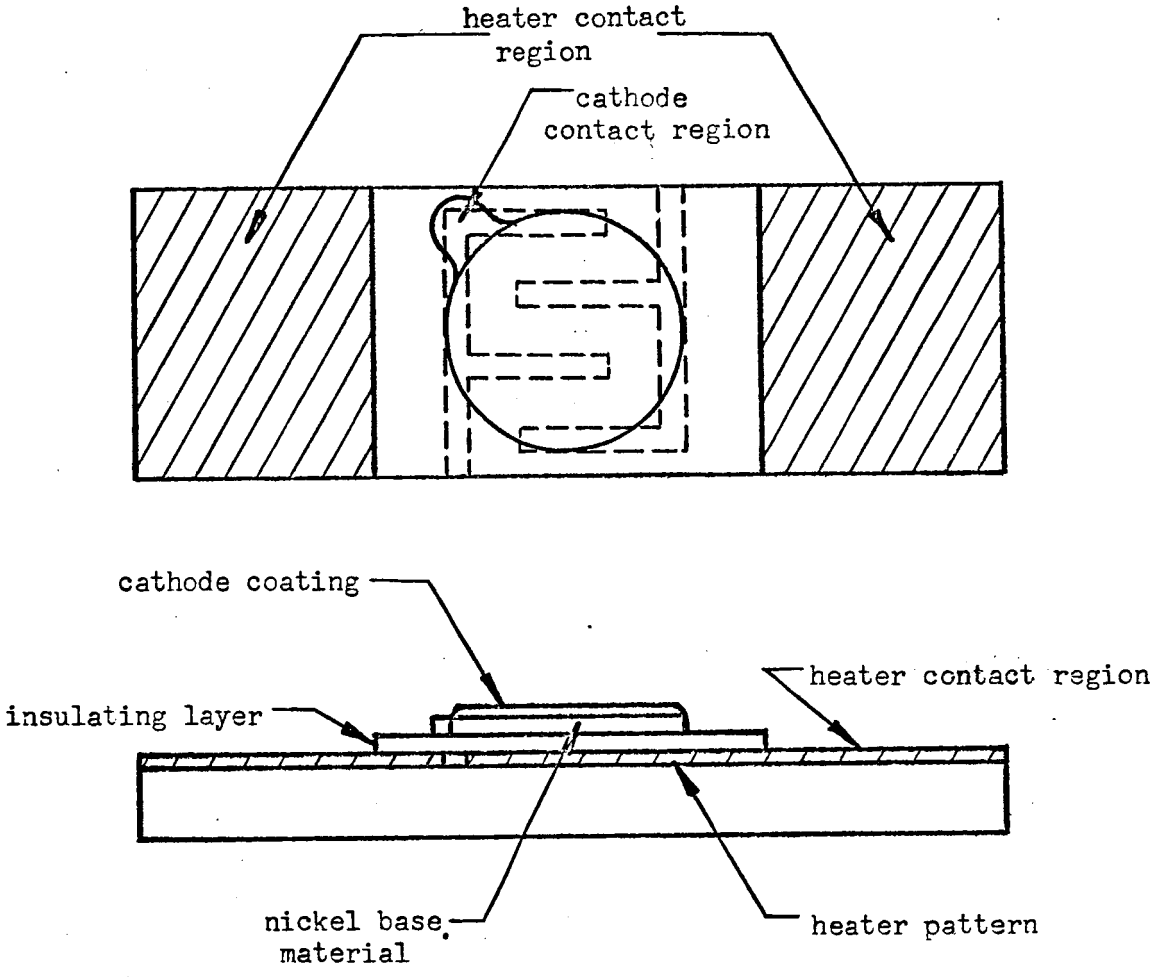

Fig. 17. Ceramic Cathode Structure

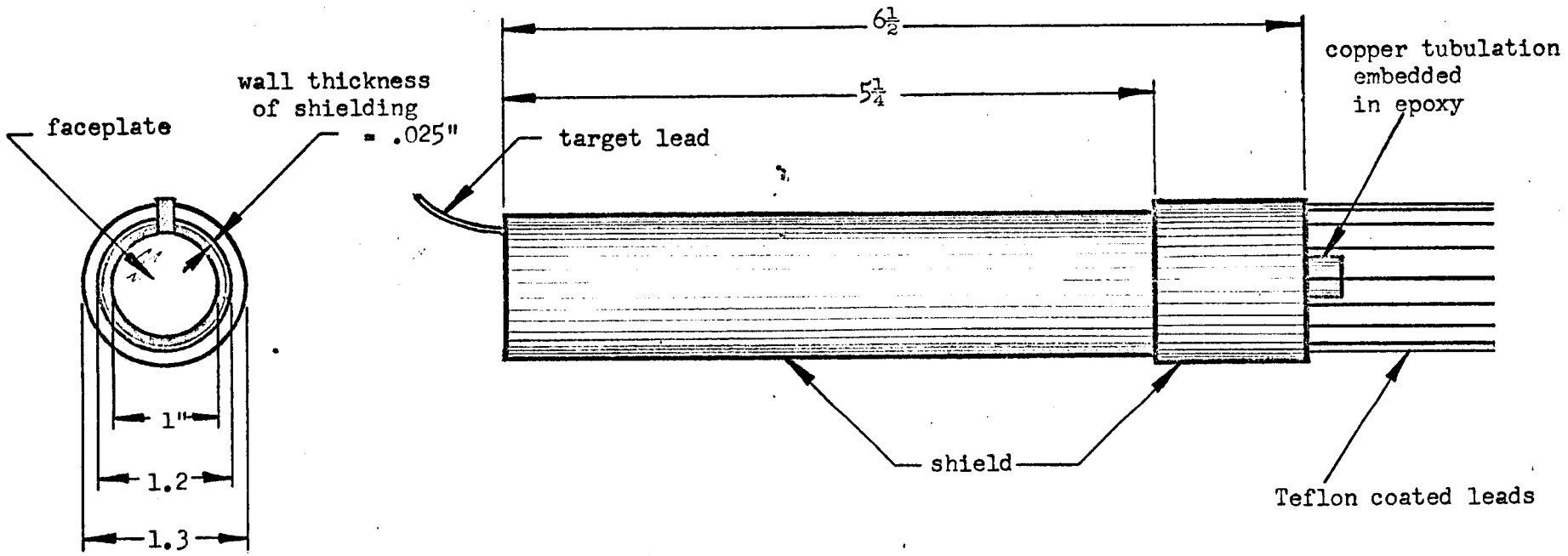

Fig. 18. External View of Ceramic Vidicon as Potted in Magnetic Shield

(a) The ceramic parts are metalized and the copper electrodes are deposited.

(b) The molybdenum pins are brazed into the ceramics.

(c) Each of the two major sections are brazed.

(d) The cathode is mounted.

(e) The two sections are joined by heliarc weld.

(f) The heater and getters are mounted and the tubulation is attached.

(g) The mesh is mounted.

(h) The faceplate is attached.

(i) The tube is pumped, the cathode is activated, the getters are flashed and the tube is pinched off.

The aforementioned production steps are discussed below in greater detail. Also discussed are some of the problems encountered which had to be solved.

(a) The standard procedure used for preparing the ceramic (alumina) surfaces for brazing is to metalize them with molybdenum and then plate nickel onto the metalizing. The molybdenum support rings and stainless steel (G_1 and G_2) electrode cups also are nickel plated while the Kovar heliarc flanges are left bare for brazing.

The electron lens and deflectron electrodes are deposited by vacuum evaporation of copper. The lens electrodes are shaped by grinding or cutting away the unwanted copper. The more complicated deflectron profile is formed by photoresist masking and etching.

Preliminary tests had shown that the brazing solder, while in the molten state, attacks the wall electrodes if it could reach them via a nickel plated surface. This difficulty was overcome by not nickel plating the metalized regions connecting the pins or brazed joints to the corresponding copper electrodes.

(b) Experience with several tubes indicated that the first set of brazed joints, which were made with a higher temperature (silver-copper-palladium) brazing alloy, tended to form brittle joints after the second braze. This may be due to the brittleness of the alloy or to a weakening of the ceramic material adjacent to the joints and it resulted in a tendency to form air leaks. Tests were therefore made to use the lower temperature

eutectic alloy of silver and copper, formerly employed only in the second braze, for both brazing operations. Since the molten alloy dissolves some of the nickel substrate, the resultant braze has a higher melting point than the original eutectic and can be kept from softening, during the second brazing cycle, by careful temperature control. This method was successful and has been used in all recent tubes.

The molybdenum pins, which are brazed into the tube wall in the first brazing operation, are held in place by a set of round metal straps.

(c) High precision stainless steel jigs are used for producing proper positioning of parts during the second braze. Oxide coatings prevent the jigs from being brazed to the tube. Considerable redesign was necessary before fully satisfactory jigging was achieved.

(d) A jig was designed for mounting the cathode subassembly accurately in the G_1 cup. A technique was evolved for attaining the desired cathode-G_1 spacing to within 0.001 inch, by means of a micrometer motion. The accurate spacing is maintained by the use of built-in welding electrodes which permit the cathode subassembly to be welded in place while being held in the mounting jig.

The success of this technique was demonstrated by the fact that the G_1 voltages for picture cutoff generally have fallen in the desired range of -45 to -110 volts.

(e) Strong and reproducible heliarc welds have been obtained once the proper conditions (surface speed, gas flow, weld current and probe spacing) had been ascertained. Argon is used as the inert atmosphere. Considerable difficulties were first encountered which were traced to the presence of silver (from the brazing joints) on the Kovar surfaces. Meticulous removal of all traces of silver was found to remove this problem.

Several tubes have been opened up (for the purpose of studying their inside condition and/or for internal repairs) by grinding open one or both of the heliarc welds. After refinishing the Kovar flanges to a smooth surface condition, it is possible to use them over again for a second welding operation.

(f) The technique developed for introducing and attaching the heater has proved to be very practical. No difficulties have been encountered in the mounting operations for the heater or getters. The tubulation section is attached, by means of a second heliarc weld similar to that described above.

(g) The electroformed nickel mesh is stretched over a nichrome ring (with a square hole) and then attached by means of a thin nichrome part which is spot welded to the ring through the mesh. It was found that in order to

obtain a taut and wrinkle-free mounting, the mesh not only has to be drawn uniformly tight but also great care must be taken in the welding operation so that no part of the mesh is exposed to excess heat. The finished mesh subassembly is mounted in the tube with four stainless steel screws.

(h) A jig was designed and built to ensure proper application of pressure during the attaching of the faceplate by means of an indium seal and to ensure proper placing of the faceplate and the target ring. Great care is required in proper preparation of the ceramic surface on which the seal is made. The surface is first ground flat and polished smooth. It has to be cleaned immediately prior to faceplate sealing to remove all particles which might cause leaks. Reliable seals have been obtained in this fashion.

(i) The tubes have been exhausted mostly on oil-free vacuum systems containing sorption and ion pumps. However, successful tubes were also pumped by means of mechanical forepumps and mercury diffusion pumps. Since the bakeout temperature has been limited to about 140°C, because of the photoconductor and indium seal, the tubes require long bake times, usually at least twelve hours.

Appropriate changes had to be made in the procedures for cathode activation and getter deposition in order to adapt them to the conditions imposed by this tube. Adequate results have been obtained; however, cathode performance has not been consistently good. The probable cause is the difficulty of proper outgassing of the gun parts and unusual thermal conditions in the ceramic tube due to the G_1-G_2 mounting arrangement.

Pinching-off of the copper tubulation generally has yielded reliable vacuum seals.

A total of twelve complete tubes were started. Six of these resulted in operable vidicons.

III. ENVIRONMENTAL TESTING AND FAILURE ANALYSIS

Suitable tests were performed on all tube parts which were considered to be potentially prone to failure due to the required sterilization or environmental conditions. The test level at which failure occurred and the mode of failure were determined, when appropriate. For the static-acceleration test a Schaevitz Model No. 'B-10-D centrifuge was used (Fig. 19). With a 4-1/2 ft. radius arm, it has a maximum acceleration capability of 200 g's.

The Ling Electronics Model No. 300 vibration unit, shown in Fig. 20, used for all vibration testing, can provide sinusoidal vibration to 100 g's peak

Fig. 19. Centrifuge for Constant Acceleration Test

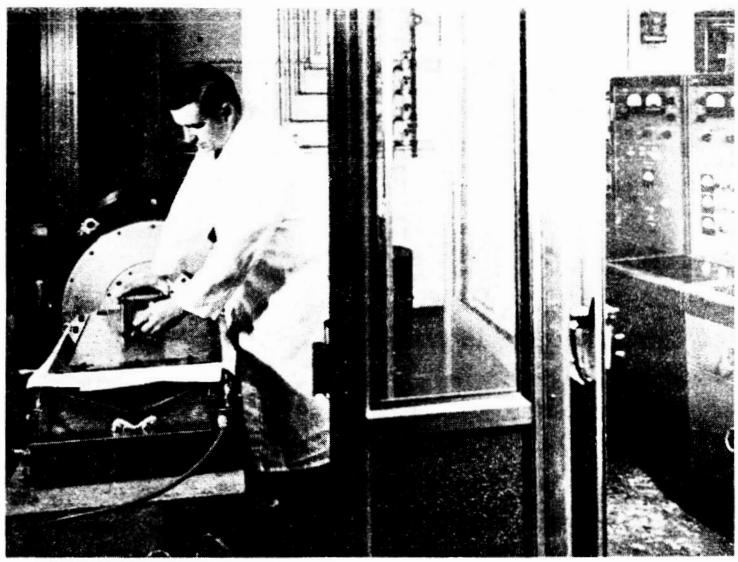

Fig. 20. Vibration Test Unit

or random vibration to 50 g's r.m.s. in the frequency range of 5 to 3000 cps. It can exert forces of up to 7000 lb. In Fig. 20 a "slippery table" is shown attached to the exciter, oriented horizontally, as used for this project.

The high acceleration shock machine, designed for testing the ceramic vidicon and its components, is shown in Fig. 21. An 8 lb. magnesium drop table, sliding on Teflon bearings, has provided impact shocks of up to 3700 g's amplitude, in a 0.45 ms half-sine pulse. At the drop height of 60 inches, a 60% rebound is obtained. The total available drop height is 76 inches. Figure 22 shows a CRO trace of a typical shock pulse. The detection circuit contains a wide-band filter passing frequencies from 200 cps to 7000 cps. The short-duration, high-g shock profile is obtained by using fiber glass material as the impact spring.

The tests made on various tube components and whole tubes are discussed below:

(a) Faceplate and Indium Seal - The resonant frequency of the faceplate subassembly is much higher than that corresponding to the shock-pulse duration. Thus no amplification of the pulse is caused and the maximum stress experienced by the faceplate and indium seal can be deduced directly from the amplitude of the pulse. The weight of the quartz faceplate is about 0.0075 lb. If the pulse height is 3000 g's, the maximum force on the indium seal is 3000 x 0.0075 or 22.5 lbs.

Static load tests were performed to establish the strength and failure mode of the indium seal on the vidicon. Two variations in sealing technique were investigated, differing in the method in which the ceramic seal surface is prepared. In the first kind of seal, the ceramic surface is ground and then metalized with molybdenum. Ten samples of indium seals formed on such a surface were tested under static loading, applied axially in the direction tending to push the faceplate away from the ceramic. The seals failed at forces varying from 75 lbs. to 270 lbs. In one case, the quartz faceplate cracked at 224 lbs. In all other samples, failure occurred due to separation of the indium seal. The average strength was 139 lbs.

The second kind of seal is formed on a bare ceramic surface which, after grinding, has been lapped smooth with a diamond compound. Six samples were tested. Three failed due to breakage of the quartz faceplate, at 161, 209 and 220 lbs., respectively. In the other three samples, the indium separated at forces of 114, 115 and 269 lbs., respectively. The average strength was 181 lbs.

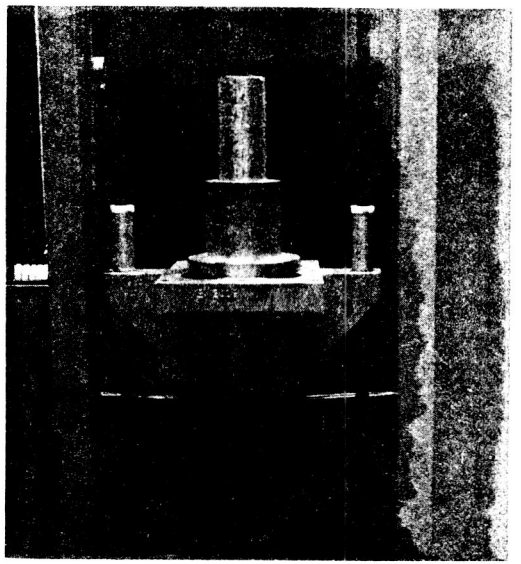

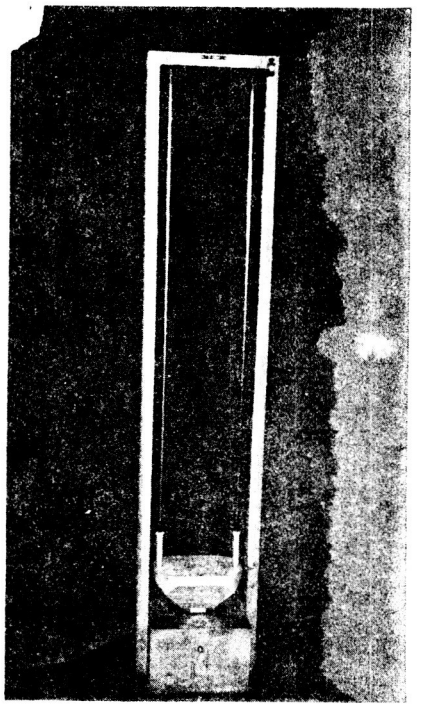

Fig. 21. High Acceleration Shock Machine and Detail of Drop Table (with holding fixture)

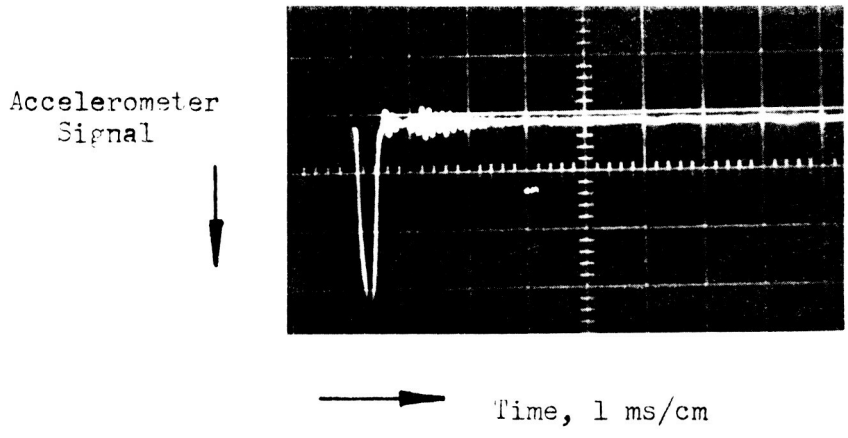

Fig. 22. Oscilloscope Trace of Typical Shock Pulse

All seals had been found to be vacuum tight.

The second technique described above, using a bare ceramic surface, was chosen for the ceramic vidicon. It promises to yield seals which are at least four times as strong as required by the tube. Actually, since in the static tests the force was applied for many seconds before failure occurred, the seals can be expected to withstand a higher momentary force as in the case of the shock pulses.

Temperature tests on the indium seal indicated that no air leaks develop if the tube is exposed to a temperature of 152°C for 24 hours. Slight leakage occurs during a 24 hour exposure at 154 to 155°C and bad leakage during a 24 hour exposure at 155 to 156°C.

(b) Mesh - The nickel ring is attached to the 0.030 inch thick molybdenum support ring by means of four No. 0-80 stainless steel screws. Tension tests on these screws screwed into molybdenum sheet of 0.025 inch thickness, indicated that they failed at about 100 lbs. due to stripping of the threads and failure of the molybdenum sheet. The weight of the mesh ring is about 3×10^{-3} lb. At an axial acceleration of 3000 g's, the total force experienced by the four screws is therefore 9 lbs. The screws, therefore, have an adequate margin of safety.

It is contemplated to sandwich a spring washer between the mesh and support ring. This would insure constant tension on each screw and reduce the probability of a screw working loose during vibration testing. Such a spring would weigh about as much as the mesh and be under an applied tension, due to the spring, of about 1 lb. per screw. Therefore, such an arrangement would still give a very high degree of safety.

Thirty-one mesh samples were tested with axial shock pulses of 3100 g's amplitude and 0.45 ms duration, five shocks being applied in each direction. Twenty-seven samples developed no wrinkles or other permanent damage. Their resonant frequency decreased by about 10% or less. The remaining four samples developed some wrinkles. However, it appears that these four samples were overstressed due to poor mounting in the testing fixture.

The resonant frequency of the mesh ranged from 2300 to 4000 cps with the average close to 3600 cps.

Shock tests were made on two subassemblies consisting of mesh support rings brazed between ceramic cylinders. Mesh rings were attached to the support rings with four screws as used in the complete tube. Each sample was exposed to five 3000 g, 0.45 ms shock in five orthogonal directions. Due to mounting limitations, the pieces were not

tested with shocks in the direction in which no force is exerted on the screws. One screw loosened in the first shock applied to it, presumably because it had not been properly tightened originally. After it was retightened, neither it nor the other seven screws showed any sign of loosening or other failure after the tests.

(c) G_1-G_2 Subassembly - Early tests on the subassembly, consisting of the G_1 and G_2 cups brazed to a 14-mil thick ceramic spacer, showed that the ceramic tended to fail in shear perpendicular to the axis. The difficulty was clearly caused by the difference in thermal expansion of the metal and ceramic parts. Two remedial steps were taken. First, the spacer was made of a stronger ceramic. Second, slots were cut in the G_1 and G_2 cups making them more flexible.

Two subassemblies of this arrangement were exposed to five 3000 g, 0.45 ms shocks in each of the six directions, without showing any damage.

A static load test was made on two G_1-G_2 subassemblies with the force applied cantilever-fashion. Both samples failed at 125 lbs., one due to breakage of the ceramic spacer, the other due to separation of the epoxy in which the samples were mounted. The shear force transmitted by the spacer during a 3000 g transverse shock is about 8.5 lbs.

One tube was found to contain a cracked ceramic spacer which, presumably, was due to the fact that this section had undergone four brazing cycles, instead of the usual single cycle. In one other case the spacer was found to be cracked immediately after the brazing operation. It is possible that this failure was the result of improper setting of the parts in the brazing jig.

In no case did a G_1-G_2 spacer, which was sound after being brazed, fail in any subsequent environmental testing.

A failure found in a tube which had been exposed to transverse shock, indicated a weakness in the brazed joint between the G_2 cup and its molybdenum support ring. This joint therefore was strengthened by enlarging the brazing surface to almost twice its previous size.

(d) Heater - The cathode heater consists of a double helix of rhenium-tungsten alloy wire just under 0.001 inch in diameter. Two straight sections of wire (the heater "legs") protrude from the cathode sleeve and are welded to two 30-mil Kovar wires. The heater is coated with alumina.

In the first of several tests, eight heater-cathode subassemblies were mounted in ceramic test units (Fig. 23) in an arrangement similar to that used in the vidicon. Four of the heaters had short legs (.050 inch long) and four had longer legs (.140 inch long). The units were exposed to five 2500 g, 0.5 ms shock pulses in each of six orthogonal directions. The four long-legged samples failed: three due to the heater having left the cathode sleeve and one due to a welded contact opening up. The four short-legged units seemed to be intact although the heaters may have shifted inside the cathode sleeve.

A second set of test samples were made which were similar to the above except that they could be life tested with the cathode, hot. Since the first test had shown up the flexibility of the bare filament wire, care was taken to leave the insulation intact up to the weld point. The units were exposed to a complete set of shocks of 2500 g amplitude and 0.5 ms duration and then to another series of 3100 g amplitude and 0.42 ms duration. This test was followed by the complete series of vibration tests. Six of the eight samples survived all tests. The two failures (one during the first shock test, the other during vibration) occurred in units having the longer legs and consisted of loss of continuity. Four of the remaining samples (three with short legs, one with long legs) were then given a life test. Power was alternately on for 55 min. and off for 5 min. The filament voltage was 8V, instead of the design value of 6.3V. The heaters were still operable when the test was terminated at over 1200 hours.

X-ray pictures taken of these units at a later date showed that two of the heaters with short legs had shifted inside the cathode sleeve. One had moved away from the cathode by an appreciable amount and would probably have given unsatisfactory performance.

The above environmental tests on heater samples had been made on heaters which had not yet undergone the cathode activation procedure. Since the recrystallization temperature of the filament wire is above the highest temperature reached during activation, it was felt that the properties of the heater would be similar before and after this process. In order to verify this assumption, eight more heater test units were made and after cathode activation, were exposed to a complete set of 3000 g shocks. All eight heaters had short legs.

Three of the heaters failed by completely leaving the cathode sleeve and opening up. Four of the remaining filaments were found to have shifted somewhat within the cathode sleeve.

In order to improve the reliability of the heater, work was started on a technique to cement the heater to the underside of the cathode.

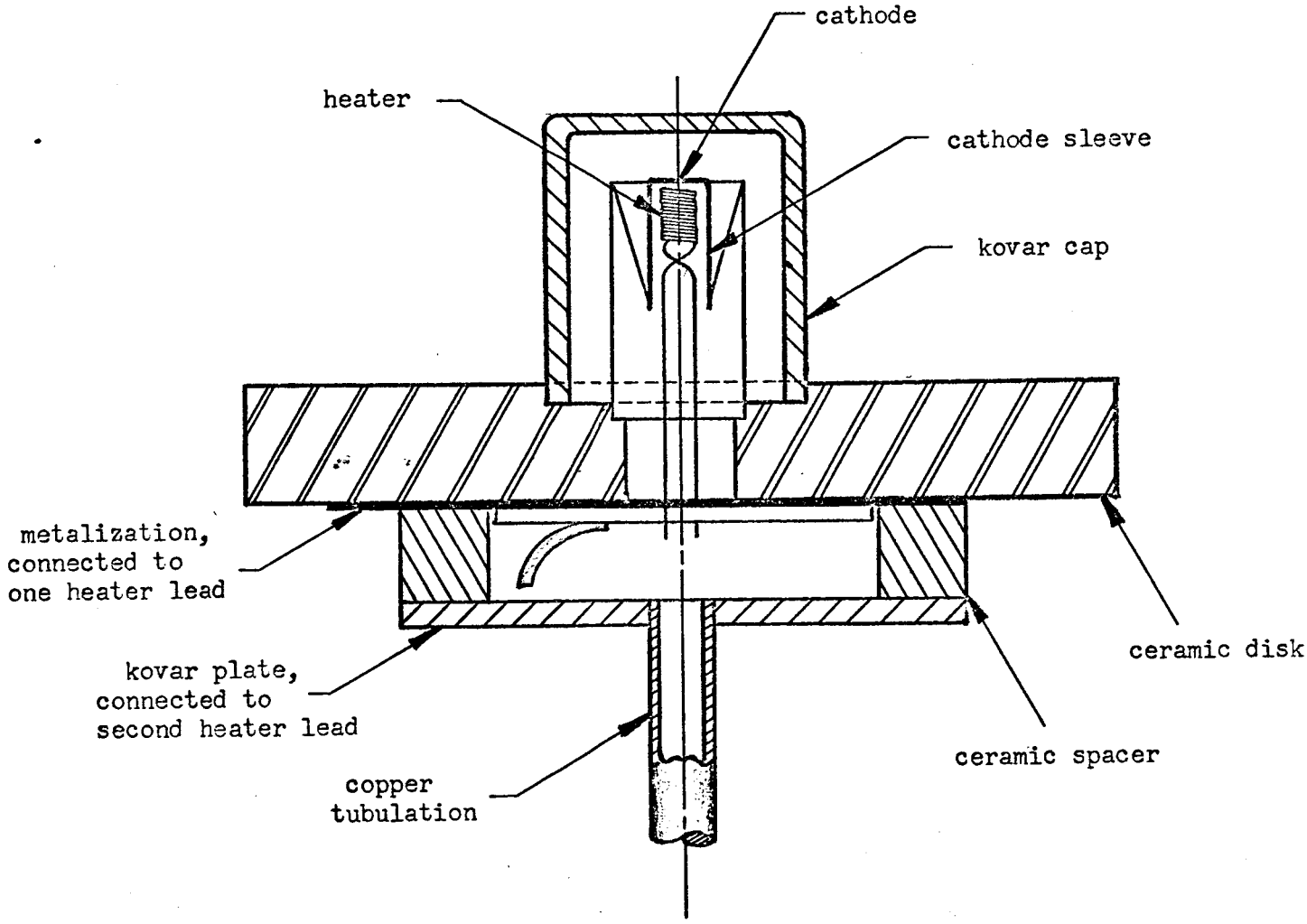

Fig. 23. Heater Test Assembly

This would prevent any appreciable motion of the heater and improve its resistance to shock and vibration substantially. It should also enhance thermal contact between heater and cathode and thus reduce the required filament power. Very encouraging results have been obtained by the use of fine nickel powder in an organic binder. The nickel sinters during the cathode activation procedure and forms a strong bond between the coated heater and the cathode base material. One test unit, with such a heater was exposed to the complete 3000 g shock and vibration test schedule and found to be undamaged. A second unit was exposed to a set of shock pulses of 3700 g amplitude without any sign of deterioration. Six more units are to be tested.

Static tension tests were made on samples of straight filament wire welded to .030 inch Kovar wire. The aforementioned welding arrangement is similar to that used in the ceramic vidicon. Failure was found to occur at about 0.2 lbs., due in all cases to fracture of the wire. If one leg has to supply the total inertial force for accelerating the whole filament at 3000 g, the transmitted force is only 0.02 lbs.

(e) Contact Pins - The molybdenum pins, used for electrical contacts through the tube wall and to brazed joints, were found to form vacuum-tight and strong bonds to the ceramic. Static loading of the pins caused failures at about 200 lbs., due to cracking of the ceramic.

(f) Magnetic Shield - Experiments were made on the magnetic shielding effect of Moly Permalloy shields before and after being exposed to shock. The four samples consisted of 0.020 inch material formed into cylinders of six inch length and 1-1/8 inch I.D. They were potted in C1100 epoxy and exposed to a complete set of 3000 g, 0.45 ms shock pulses.

Shielding efficiency was measured in an applied field of 90 gauss. The field observed inside the shield was found to be about 0.6 gauss initially and had a maximum value of 1.5 gauss after the shock test. Thus the shielding efficiency was still above 98%.

(g) Potting Compounds - Most of the potting compounds tested were found to have insufficient stiffness. The durometer reading of the compound should be at least 80 in order that the potted tube has a resonant frequency of 3000 cps or above as required. Epoxy which would satisfy this requirement, has an excessive thermal expansion coefficient which might cause damage to the tube at low temperatures.

A preliminary search indicated polyurethane to be the most promising material as far as stiffness and resistance to the sterilization procedures are concerned. Test samples were made of several formulations of this material with metal rods potted within metal tubes simulating the

actual tube arrangement. PR1538 (Product Research Co.), cured at about 90°C for eight hours, was found to have acceptable elastic characteristics and to be able to withstand the dry-heat and ethylene-oxide sterilization procedures without appreciable change in physical properties. Samples of this material also were exposed to air at 160°F and relative humidity of 95% for 3 days without apparent changes.

Since it is desirable to use a potting compound of considerably greater stiffness than the minimum durometer value of 80 mentioned above, tests were made on PR 1538 to which various amounts of fine glass spheres (30 to 300 microns in diameter) had been admixed. Encouraging increases in stiffness have been obtained, but problems remain concerning proper mixing without inclusion of air bubbles and concerning the heat resistance of the resultant material.

(h) Complete Tube - A prototype ceramic bottle was made to indicate whether the various types of joints, used in the tube, are impervious to the ethylene oxide decontamination gas. The ionization gage which had been incorporated in the unit, showed that no perceptible trace of the gas was allowed to penetrate the bottle.

In the first environmental test of a potted tube, a mechanical sample was used which did not contain a mesh or a heater. Thirty shocks (five along each of the six directions) of 3000 g amplitude and 0.45 millisecond duration were applied without causing apparent damage. The resonant frequency in the axial direction was found to be in excess of 3000 cps.

Three potted tubes were exposed to nearly square shock pulses, of at least 3200 g amplitude and one-half millisecond duration in tests performed at the Jet Propulsion Laboratories. Two of the tubes were incomplete internally while the third was an operative vidicon. Altogether these tubes were exposed to thirteen transverse and six axial shocks.

No damage was found on the body of any of these tubes. The complete vidicon failed during the fifth transverse shock without having received any shock in the axial direction. The failure consisted of an open filament and of a distortion of the G_2 cup structure. It is believed that the break in the heater, which occurred adjacent to the weld at the support wire, was caused by the motion resulting from the failure at the G_2 cup.

As has been mentioned above, the braze area between the G_2 cup and its support ring has since been increased considerably.

Experimental tests on the behavior of the ceramic vidicon under shock-pulse excitation indicated that the acceleration experienced by the

tube components is significantly greater than that applied to the fixture which holds the tube. The resonant frequency of the tube as mounted in the potting compound is about 3000 cps. The frequency corresponding to the 0.45 ms pulse duration is 2200 cps. These two frequencies are sufficiently close, that a shock pulse applied to the magnetic shield causes an acceleration of tube tube which is greater than the applied acceleration by a factor of about 1.4.

Due to the flexibility inherent in the Kovar joint at the gun of the tube (see Fig. 16), the amplification factor for the lower tube section is even larger. This is particularly true for transverse shocks in which the lower section is deflected in cantilever fashion. The amplification factor in this case is about 2.5.

As a final test for the period of this report, a potted ceramic vidicon was exposed to a complete environmental test. The tube was first given an operational test which was repeated after the prescribed constant-acceleration and sinusoidal and random vibration tests. The tube was then exposed to five shock pulses in each of the six directions. These pulses were half-sinusoidal with 0.45 ms duration. The amplitude of the applied transverse shocks was 1200 g and of the axial shocks 2800 g. Presumably, therefore, all the accelerations experienced by the heater, as well as the axial accelerations of the mesh, were about 3000 g's. These, of course, are the critical aspects of the tube.

The pursuant operational test gave no indication of any deterioration.

The tube will be put through the gas and dry-heat sterilization procedures and will then be tested at higher shock levels than before.

A similar tube was delivered to JPL at the end of this Interim Report period.

IV. PERFORMANCE

As an example of the characteristics of an electrostatic ceramic vidicon, the results of measurements on the most recent tube are given. This tube is similar to the previous samples, except that a 1/2 inch electrode section was added between deflectron and mesh in order to improve beam landing and deflection sensitivity. It was somewhat better in performance than the other tubes, but had similar resolution. It has not been exposed to any sterilization treatments.

All measurements were made under standard (60 frames/second) television operation, without aperture correction. Figure 24 shows dark current as a function of target voltage, and Fig. 25 gives signal current, at a faceplate

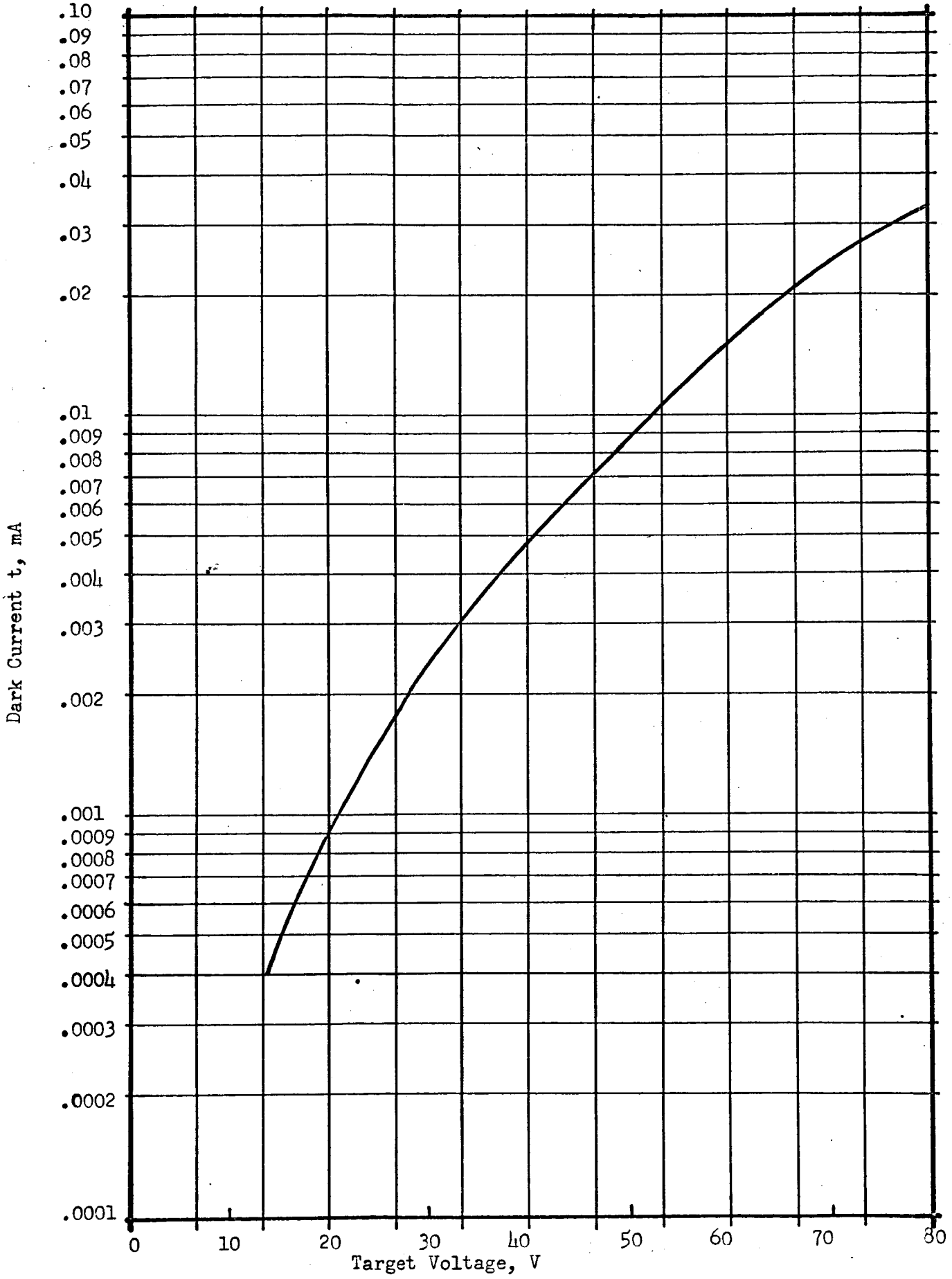

Fig. 24. Dark Current Vs. Target Voltage for Ceramic Vidicon

Tube M

Faceplate Illumination = 1.0 fc.

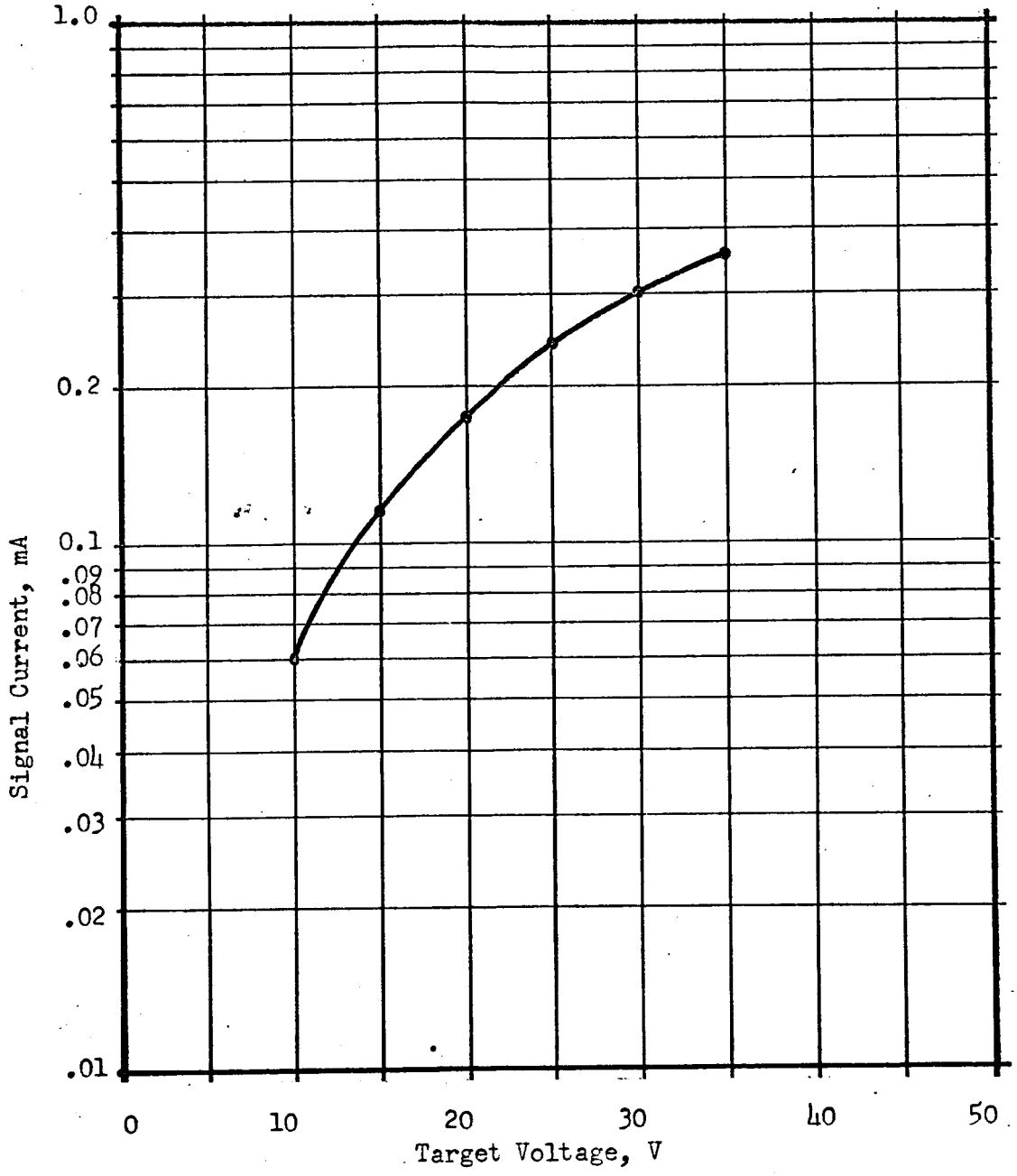

Fig. 25. Signal Current Vs. Target Voltage for Ceramic Vidicon

illumination of 1.0 footcandle, versus target voltage. Both plots are semilogarithmic. Figure 26 is a logarithmic graph of signal current versus faceplate illumination for a target voltage of 20V. The vidicon has a gamma of 0.67.

Figure 27 depicts the spectral response of the tube. The experimental values were adjusted to yield the signal current corresponding to the same amount of luminant power incident on the faceplate at all wavelengths. The sensitivity peaks near 570 mu. The relatively high values at the shorter wavelengths are believed to be spurious, probably because of transmission of infrared or ultraviolet radiation by the optical filters.

The tube resolves at least 550 television lines in the center of the raster and 500 lines in the corners. At least nine gray-scale steps can be distinguished.

The horizontal square-wave response of the vidicon is presented in Fig. 28. The equivalent line number, N_e, corresponding to this characteristic is 267 lines.

A typical set of operating voltages is the following:

Target	20V
G_1	-50
G_2	400
G_3	350
G_4	60
G_5	350
Center of deflectron	400
Mesh	700

V. SUMMARY AND CONCLUSIONS

The photoconductive layers made during Task I were evaluated in the commercial 7735A type vidicon. Performance characteristics studied consisted of

(a) Dark current vs. target voltage,
(b) Signal current (at constant, uniform illumination) vs. target voltage,
(c) Signal current (at constant target voltage) vs. illumination,
(d) Spectral response,
(e) Ultimate resolution,
(f) Gray-scale rendition,
(g) Lag.

The tubes were tested for some or all of these characteristics before and after the dry-heat sterilization procedure which consisted of three 36-hour 145°C bakes in dry nitrogen. In addition, many tubes were tested following the first bake, and some also after the second.

Tube M

Target Voltage = 20V
Dark Current = .001 mA

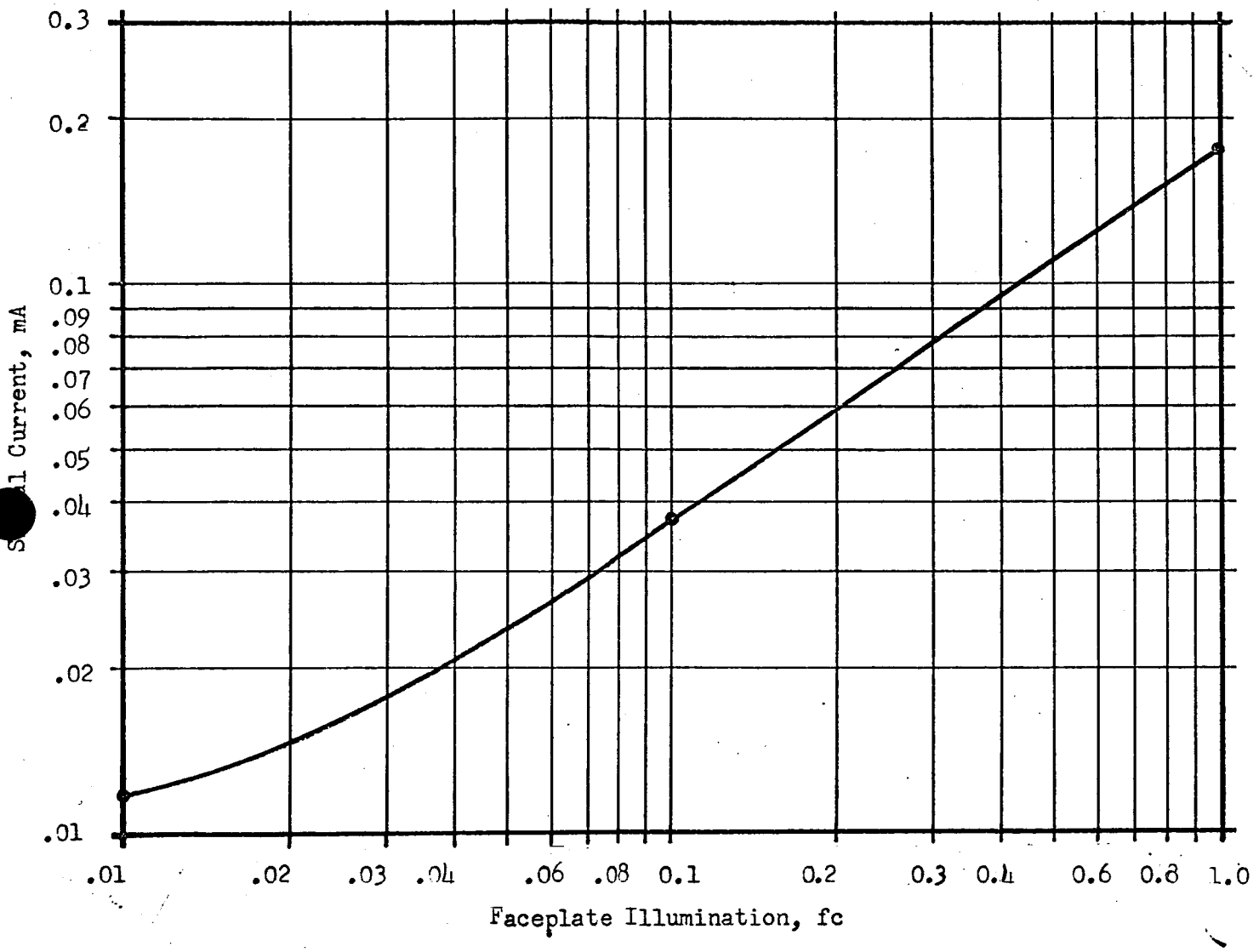

Fig. 26. Signal Current Vs. Faceplate Illumination for Ceramic Vidicon

Tube M

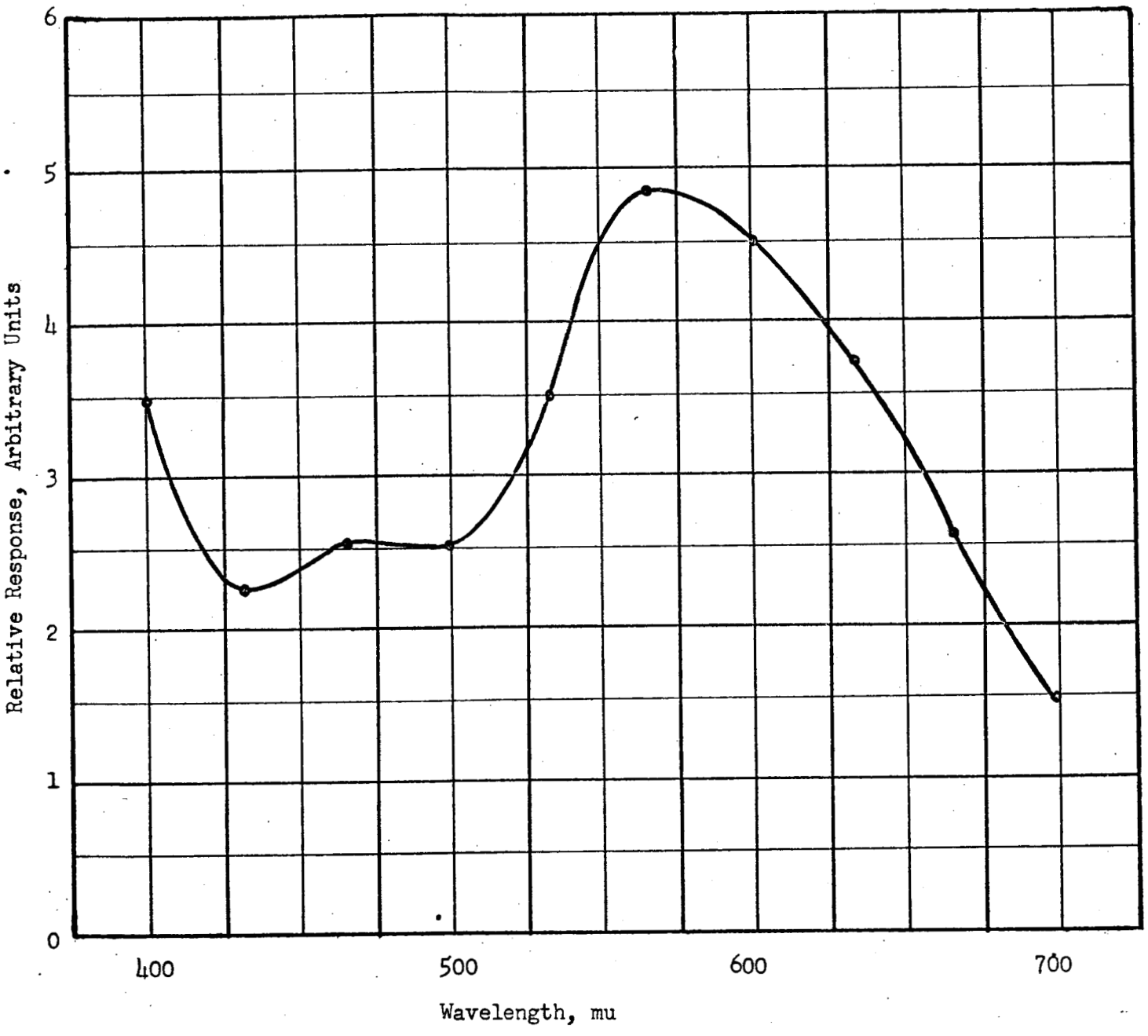

Fig. 27. Spectral Response of Ceramic Vidicon

Tube M

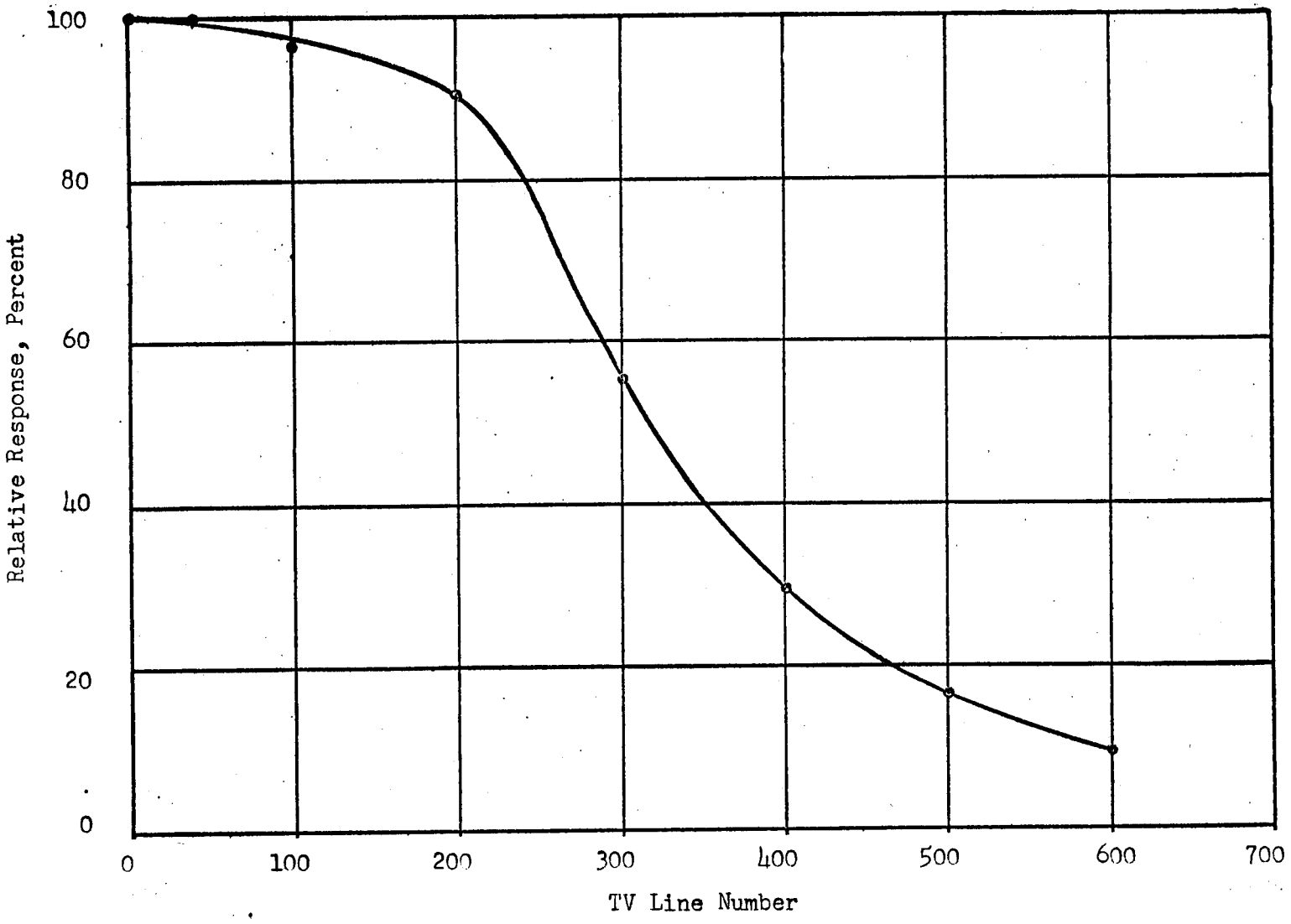

Fig. 28. Amplitude Response of Ceramic Vidicon

In testing, primary consideration was given to the dark current and signal current characteristics and, to some degree, resolution. No significant changes, from tube to tube or from before to after sterilization, were observed in either gray-scale rendition or lag characteristics. In some tubes, sterilization caused a perceptible change in the shape of the spectral response curve but not of sufficient degree to be of significance in this program.

The major effect of the sterilization procedure on tube characteristics consisted of an increase in dark current and a smaller increase in signal current. These changes varied considerably from tube to tube. On the average, the dark current at 20V target voltage approximately doubled and the signal current increased by about 25%.

While the resolution in most tubes did not change much during sterilization, several tubes did show an appreciable loss while a few exhibited an increase.

Most of the tubes showed some spurious signal (spots). It was found that this problem can be greatly reduced by proper cleaning of the faceplates prior to the photoconductor evaporation. In no instance did sterilization cause an increase in spottiness.

At the beginning of this project the slow-scan photoconductor used was found to be suitable for sterilization. Only a minor adjustment in its chemical composition was made, in order to cause a small decrease in dark current. The major portion of the work in Task I consisted of improvements in freedom from spurious signals and of obtaining experimental data for establishing the characteristics of the photoconductor.

In Task II it was demonstrated that an operable vidicon can be built which is capable of good performance as well as being able to withstand sterilization procedures and severe environmental testing.

The tube design is based on a ceramic-metal modular construction. Electrostatic focusing and deflection are employed with the deflectron, an integral portion of the ceramic envelope. The tube is potted in a polyurethane compound within a Moly Permalloy magnetic shield.

Early efforts were directed at developing techniques for making strong and vacuum-tight brazed joints while maintaining precise positioning of the tube parts. Best results were obtained by use of a single (silver-copper) brazing alloy for the two consecutive brazes.

The quartz faceplate is attached with an indium seal. Mechanically tensioned, unfired, nickel mesh was found to be the most rugged electroformed mesh material as far as resistance to vibration and shock are concerned. The low-power gun is made in a brazed construction and a technique is under development for cementing the heater to the underside of the cathode.

Continual emphasis was put on ensuring the reliability of the tube under environmental testing. All critical components and subassemblies were tested and an effort was made to anticipate all possibilities of eventual failure.

The performance of the tube is very encouraging. It is expected that when the activation of the cathode has been optimized, a further improvement in performance characteristics will result.

A prototype model of the vidicon was delivered to JPL.